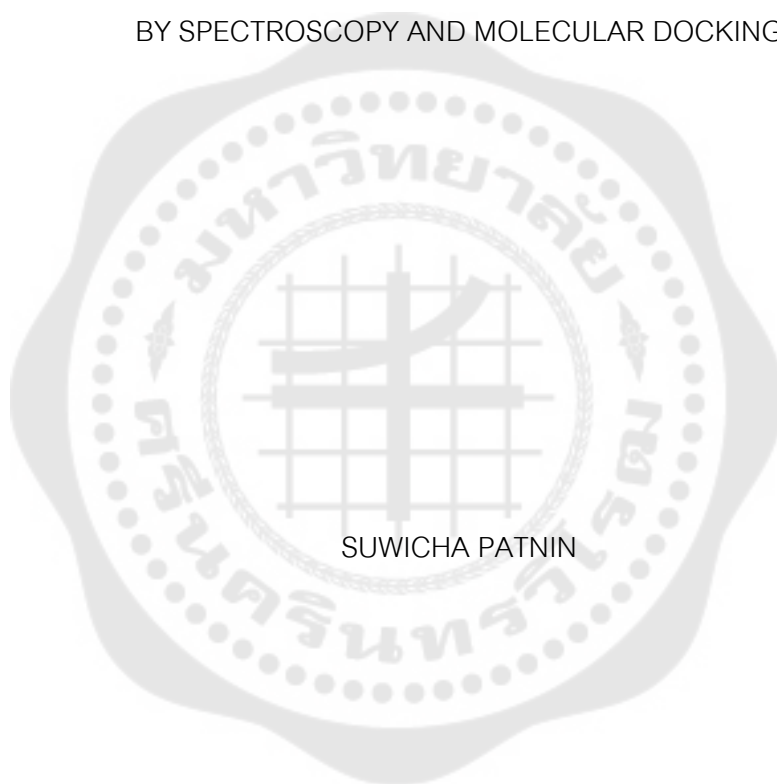




BINDING INTERACTION BETWEEN SERUM ALBUMIN WITH QUINOLINE DERIVATIVES
BY SPECTROSCOPY AND MOLECULAR DOCKING



Graduate School Srinakharinwirot University

2020

การศึกษาอันตรกิริยาระหว่างโปรตีนซีรัมอัลบูมินกับสารประกอบเชิงซ้อนควิโนลีนด้วยวิธี
สเปกโทรสโกปีและโมเลกุลาร์ดอกกิ้ง



ปริญญานิพนธ์นี้เป็นส่วนหนึ่งของการศึกษาตามหลักสูตร
ปรัชญาดุษฎีบัณฑิต สาขาวิชาเคมีประยุกต์
คณะวิทยาศาสตร์ มหาวิทยาลัยศรีนครินทรวิโรฒ
ปีการศึกษา 2563
ลิขสิทธิ์ของมหาวิทยาลัยศรีนครินทรวิโรฒ

BINDING INTERACTION BETWEEN SERUM ALBUMIN WITH QUINOLINE DERIVATIVES
BY SPECTROSCOPY AND MOLECULAR DOCKING



SUWICHA PATNIN

A Dissertation Submitted in Partial Fulfillment of the Requirements
for the Degree of DOCTOR OF PHILOSOPHY
(Applied Chemistry)

Faculty of Science, Srinakharinwirot University

2020

Copyright of Srinakharinwirot University

THE DISSERTATION TITLED
BINDING INTERACTION BETWEEN SERUM ALBUMIN WITH QUINOLINE DERIVATIVES
BY SPECTROSCOPY AND MOLECULAR DOCKING

BY
SUWICHA PATNIN

HAS BEEN APPROVED BY THE GRADUATE SCHOOL IN PARTIAL FULFILLMENT
OF THE REQUIREMENTS FOR THE DOCTOR OF PHILOSOPHY
IN APPLIED CHEMISTRY AT SRINAKHARINWIROT UNIVERSITY

(Assoc. Prof. Dr. Chatchai Ekpanyaskul, MD.)
Dean of Graduate School

ORAL DEFENSE COMMITTEE

..... Major-advisor Chair
(Assoc. Prof. Apinya Chaivisuthangkura)	(Asst. Prof. Patchareenart Saparpakorn)
..... Co-advisor Committee
(Asst. Prof. Mayuso Kuno)	(Assoc. Prof. Siritron Samosorn)
..... Co-advisor	
(Arthit Makarasen)	

Title	BINDING INTERACTION BETWEEN SERUM ALBUMIN WITH QUINOLINE DERIVATIVES BY SPECTROSCOPY AND MOLECULAR DOCKING
Author	SUWICHA PATNIN
Degree	DOCTOR OF PHILOSOPHY
Academic Year	2020
Thesis Advisor	Associate Professor Apinya Chaivisuthangkura
Co Advisor	Assistant Professor Mayuso Kuno
Co Advisor	Arthit Makarasen

The intermolecular interaction between quinoline derivatives, 2, 4-disubstituted quinolines, with bovine serum albumin (BSA) and human serum albumin (HSA) was investigated under physiological conditions. UV-Vis spectrophotometry, fluorescence spectroscopy, competitive binding experiments and molecular docking were used for the binding studies. The fluorescence of the protein was quenched by these quinoline derivatives through a static quenching mechanism, with the number of binding sites (n) of approximately 1. The binding constants (K_b) ranged from 10^4 - 10^5 L.mol⁻¹ at three different temperatures (298, 308 and 318 K). The binding interaction was spontaneous and the changes in enthalpy (ΔH) and entropy (ΔS) were 48.5 kJ mol⁻¹ and -65.21 J mol⁻¹ K⁻¹, respectively for BSA, and -44.55 kJ mol⁻¹, -51.89 J mol⁻¹ K⁻¹, respectively for HSA, indicating that the interaction could be van der Waals force and/or hydrogen bonding interaction. Site marker competitive experiments suggested the binding site at site I (sub-domain IIA), and molecular docking supported the spectroscopic results. This study can provide more information for the development of the appropriate quinoline structure to obtain more effective reagent against HIV-1 RT inhibitor.

Keyword : Quinoline derivatives Serum albumin UV-Vis spectrophotometry Fluorescence spectroscopy Molecular docking

ACKNOWLEDGEMENTS

I have been deeply motivated and inspired from numerous people who have helped me in interminable ways to complete this thesis. First and foremost, I would like to express my deep and sincere to my thesis advisor, Assoc. Prof. Dr. Apinya Chaivisuthangkura, who has distributed generous support and provided invaluable guidance throughout my stay at Srinakharinwirot University. I am extremely thankful for what her has offered me for the intellectual freedom to work on whatever research I found interesting. I consider myself very blessed to have been a part of her research group. I am very appreciative of the good companionship that I have enjoyed in the lab. Thanks to both past and present members of the group with whom I have had a chance to interact.

I would also like to manifest my deep and sincere thanks to my thesis advisor, Assoc. Prof. Dr. Apinya Chaivisuthangkura and Asst. Prof. Dr. Mayuso Kuno for their invaluable help and constant encouragement throughout the course of this research. I am most appreciative for their enlighten and counseling, not only the research methodologies but also many other methodologies in life. This thesis would not have been accomplished without all the support that I have always achieved from them.

In addition, I am grateful for the senior researcher of Chulabhorn Research Institute: Dr. Arthit Makarasen for imputation and his help. Finally, I most gratefully acknowledge my parents and my friends for all their support and valuable prayers throughout the period of this research.

SUWICHA PATNIN

TABLE OF CONTENTS

	Page
ABSTRACT	D
ACKNOWLEDGEMENTS.....	E
TABLE OF CONTENTS.....	F
LIST OF TABLE.....	I
LIST OF FIGURE.....	J
CHAPTER I INTRODUCTION.....	1
Background.....	1
Objectives of the research.....	3
Significance of the research	4
Scope of the research.....	4
CHAPTER II THEORY AND LITERATURE REVIEWS	5
Amino acids	5
Proteins.....	9
UV-VIS spectroscopy	12
Fluorescence spectroscopy	15
The fluorescence quenching mechanisms	16
Thermodynamic parameters and binding model	18
The binding site of ligand on BSA and HAS.....	19
Computational chemistry	20
Molecular docking	20
Related research.....	22

Antimalarial activity.....	22
Anti-inflammatory activity	24
Antibacterial.....	24
Antineoplastic	25
Antifungal.....	26
Antiviral	26
Anti-HIV.....	27
CHAPTER III EXPERIMENTAL.....	34
Equipment.....	34
Chemical reagents.....	34
Methods.....	35
UV spectra measurements.....	35
Fluorescence quenching measurements	35
Binding constant and number of binding site.....	35
Thermodynamic parameters and binding model	35
Competitive binding experiments	36
Molecular docking	36
CHAPTER IV RESULTS AND DISCUSSION.....	37
UV-Vis Spectra	37
Fluorescence quenching measurements	39
Binding constant and number of binding site	44
The thermodynamic parameter and the binding mode	46
Competitive binding between (1), warfarin and ibuprofen to serum albumin.	50

Molecular docking of compounds 1 and 2 with serum albumin	51
Molecular docking of 2,4-disubstituted quinoline derivatives with serum albumin	56
CHAPTER V Conclusion	70
REFERENCES.....	72
VITA	77



LIST OF TABLE

	Page
Table 1 Stern–Volmer quenching constants of serum albumin with compound 1 at three different temperatures.	43
Table 2 Stern–Volmer quenching constant of BSA and HSA with compound 2 at three different temperature system.	43
Table 3 Binding constants and the number of binding site of serum albumin with (1) at three different temperatures.....	45
Table 4 Binding constants and the number of binding site of serum albumin with (2) at three different temperatures.....	46
Table 5 The parameters of thermodynamic of the binding between BSA and (1).....	48
Table 6 The parameters of thermodynamic of the binding between HSA and (1).	49
Table 7 The thermodynamic parameter of the binding between BSA and (2).	50
Table 8 The thermodynamic parameters of the binding between HSA and (2).	50
Table 9 Binding constants of serum albumin with (1) in the presence of the site markers.	51
Table 10 Binding constants of serum albumin with (1) in the presence of the site markers.....	51
Table 11 Binding energy (BE) of serum albumin with (1) and (2) by using molecular docking.....	52
Table 12 Inhibitory activity (%) of the 2,4-disubstituted quinoline derivatives (1 μM) against HIV-1 RT.....	58
Table 13 Binding energy of serum albumin with 2,4-disubstituted quinoline derivatives by using molecular docking	59

LIST OF FIGURE

	Page
Figure 1 Quinoline structure	1
Figure 2 4-(4'-cyanophenoxy)-2-(4''-cyanophenyl)-aminoquinoline	3
Figure 3 4-(4'-cyanophenoxy)-2-(5''-cyanopyridinyl)-aminoquinoline.....	3
Figure 4 Basic structure of amino acid	5
Figure 5 Zwitterion	6
Figure 6 Aromatic amino acids	6
Figure 7 Polar uncharged amino acids.....	7
Figure 8 Nonpolar amino acids	7
Figure 9 Positive charged amino acids.....	8
Figure 10 Negative charged amino acids	8
Figure 11 Peptide bond of amino acids.....	9
Figure 12 Four structures of proteins	11
Figure 13 Schematic diagram of electromagnetic spectrum	12
Figure 14 The electronic transition.....	13
Figure 15 The absorption spectrum of aromatic amino acids.....	15
Figure 16 The transitions between electronic states of a molecule	16
Figure 17 the quenching mechanism	17
Figure 18 The locations of domain-binding sites of HSA (left) and BSA (right)	20
Figure 19 The lock and key theory.....	21
Figure 20 Comparison of docking and reverse docking.....	22
Figure 21 Bisquinoline compounds	23

Figure 22 2-methyl-6-ureido-4-quinolinamides	23
Figure 23 The structure quinolone derivative	24
Figure 24 3-benzyl-6-bromo-2-methoxy-quinolines.....	25
Figure 25 3-Amido-4-anilinoquinolines	25
Figure 26 2-chloroquinoline derivatives	26
Figure 27 Anilidoquinoline derivative	26
Figure 28 1-benzyl-1H-1,2,3-triazole derivatives	27
Figure 29 The new HIV-1 reverse transcriptase inhibitors.....	28
Figure 30 benzofurano[3,2-d]pyrimidin-2-ones	29
Figure 31 the compounds A1 and A11	29
Figure 32 Amino-oxydiarylquinoline Derivatives.....	30
Figure 33 Alprazolam	31
Figure 34 Zonisamide.....	31
Figure 35 Tussilagone	32
Figure 36 Clonazepam	33
Figure 37 UV-VIS spectra of BSA (A) and HSA (B) with increasing the concentration of (1) (a-f). The concentration of serum albumin was kept at 6 μM with increasing the concentration of quinoline derivatives (1) (0, 10, 20, 30, 40, and 50 μM).	38
Figure 38 UV-VIS spectra of BSA (A) and HSA (B) with increasing the concentration of (2) (a-f). The concentration of serum albumin was kept at 5 μM with increasing the concentration of quinoline derivatives (1) (0, 10, 20, 30, 40, and 50 μM).	39
Figure 39 The emission spectra of BSA (A) and HSA (B) with the increasing concentration of (1).	41

Figure 40 The spectra of BSA (A) and HSA (B) with the increasing concentration of (2).	42
Figure 41 Plot of the quenching interaction of BSA (A) and HSA (B) with (1).....	44
Figure 42 Plot of the quenching interaction of BSA (A) and HSA (B) with (2).....	45
Figure 43 Van't Hoff plot for the binding interaction of BSA with (1) (A), and HSA with (1) (B).....	48
Figure 44 Van't Hoff plot for the binding of BSA with (2) (A), and BSA with (2) HSA (B).	49
Figure 45 (A) The conformation of (1) of BSA. (B) The amino acids of BSA.....	53
Figure 46 (A) The conformation of (1) of HSA. (B) The amino acids of HSA.	54
Figure 47. (A) The conformation of 4 (2) of BSA. (B) The amino acids of BSA.....	55
Figure 48. (A) The conformation of (2) of BSA. (B) The amino acid of HSA.	55
Figure 49 The structures of quinoline derivatives.....	57
Figure 50 (A) The conformation of compound 3 of BSA. (B) The amino acids on BSA...	60
Figure 51 (A) The conformation of compound 3 of HSA. (B) The amino acids on HSA. .	61
Figure 52 (A) The conformation of compound 4 of BSA. (B) The amino acids on BSA...	62
Figure 53 (A) The conformation of compound 4 of HSA. (B) The amino acids on HSA. .	62
Figure 54 (A) The conformation of compound 5 of BSA. (B) The amino acids on BSA...	63
Figure 55 (A) The conformation of compound 5 of HSA. (B) The amino acids on HSA. .	64
Figure 56 (A) The conformation of compound 6 of BSA. (B) The amino acids on BSA...	65
Figure 57 (A) The conformation of compound 8 of HSA. (B) The amino acids on HSA. .	66
Figure 58 (A) The conformation of compound 7 of BSA. (B) The amino acids on BSA...	67
Figure 59 (A) The conformation of compound 7 of HSA. (B) The amino acids on HSA. .	67
Figure 60 (A) The conformation of compound 3 of BSA. (B) The amino acids on BSA...	68
Figure 61 (A) The conformation of compound 8 of HSA. (B) The amino acids on HSA. .	69



CHAPTER I

INTRODUCTION

Background

Quinoline is nitrogen comprising the heterocyclic aromatic compound. Quinoline, C₉H₇N (Figure 1), is an alkaloid from various plant species. Quinoline has a molecular weight of 129.16, which is colorless hygroscopic liquid with a strong smell. The log P value is 2.05 with pK_b and pK_a of 4.86 and 9.6, respectively., (Abadi, Hegazy, & El-Zaher, 2005). Quinoline is insoluble in cold water but is well soluble in hot water and other organic solvents. It can cause both substitution reactions. electrophilic and nucleophilic. Quinoline is mainly used as a core structure to synthesize pharmacologically active substances and other special chemicals. It is also non-toxic to humans when absorbed through the mouth and inhalation. (Narayan Acharya, Thavaselvam, & Parshad Kaushik, 2008, pp. 487-494).

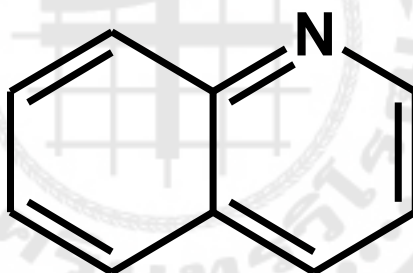


Figure 1 Quinoline structure

Many results have found that quinoline derivatives show numbers of biological and pharmacokinetic activities including antitubercular (Ciprofloxacin and Moxifloxacin), antibacterial (Ciprofloxacin), anticancer and antimalarial (Quinine, Quinidine), antifungal (Clioquinol) and antiviral (Saquinavir). Besides, WHO has recommended Ciprofloxacin and Moxifloxacin for anti-tuberculosis drugs (Paul, Guchhait, & Bhattacharya, 2017). Quinoline derivatives can be transported in the blood through merging with albumin. Serum albumin is the most common protein in human plasma, is the transport protein in the human body. Serum albumin is the most abundant protein in human plasma and is

the protein that is transported in the human body. Serum albumin has a significant function in binding to circulating medicines. The serum albumin's binding relationship with the drug plays a role to in vivo drug transmission and biological metabolism. Thus, The study of the binding relationship between drug molecules and serum albumin is very useful for further understanding of the mechanism of drug action (Shi, Chen, Wang, Zhu, & Wang, 2015, pp. 630–637).

BSA or Bovine serum albumin is a residue of 583 and HSA is a residue of 585. Both the HSA and BSA have three similar domains (represented as I, II, and III) that make up the heart-shaped molecules. Each domain comprises two subdomains (A and B), in which BSA and HSA have similar sequence, shape, and configuration. BSA has two residues of TRP (Trp-134 and Trp-213) and HSA has one residue of TRP (Trp-214) with a strong intrinsic fluorescence. BSA and HSA have used extensively as model proteins for testing the binding relationship between drugs and serum albumin (C. Carter & X. Ho, 1994, pp. 153-176).

The objective of this thesis is to investigate the mechanism of binding interaction of quinoline derivatives such as (4'-cyanophenoxy)-2-(4''-cyanophenyl)-aminoquinoline (1) and (4'-cyanophenoxy)-2-(4''-cyanopyridinyl)-aminoquinoline (2) (Figure 2,3) with BSA and HSA. (1) and (2) have been designed and synthesized by A. Makarasen and coworker [6]. (1) and (2) have been demonstrated Inhibiting anti-HIV-1 RT activities. (1) has shown percentage inhibitory activity at a similar level to that of Nevirapine (NVP) used for Non-nucleoside reverse transcriptase inhibitors (NNRTIs) (Makarasen et al., 2019, pp. 671-682). The results showed binding constant (K_b), quinoline derivatives-BSA complex binding site and binding energy. This research performed fluorescence spectroscopy, UV-VIS spectroscopy, and molecular docking methods. It can be concluded that his research would provide essential knowledge to explain the binding mechanisms of serum albumin quinoline derivatives to better understand the transportation of quinoline derivatives in vivo.

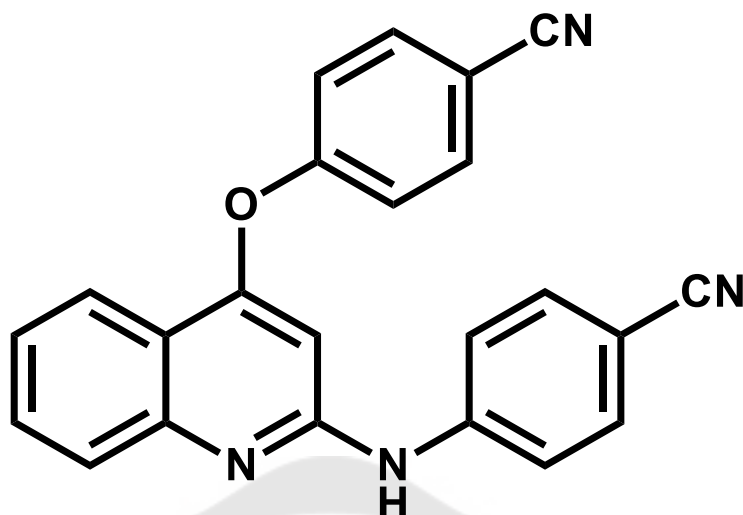


Figure 2 4-(4'-cyanophenoxy)-2-(4''-cyanophenyl)-aminoquinoline

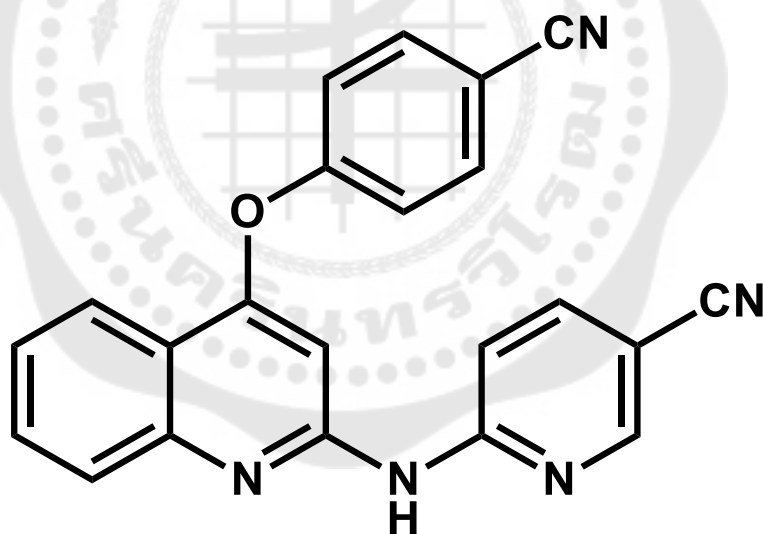


Figure 3 4-(4'-cyanophenoxy)-2-(5''-cyanopyridinyl)-aminoquinoline

Objectives of the research

1. To study the binding interaction between quinoline derivatives with protein.
2. To study the binding site of proteins and binding energy for the binding of quinoline derivative with protein by molecular docking.

3. To determine the thermodynamic parameters for the binding processes.
4. To compare binding efficiency between compound (1) and compound (2) with proteins.

Significance of the research

1. Obtain the binding constants between quinoline derivatives with protein.
2. Obtain the quenching mechanism between quinoline derivatives with protein.
3. Obtain the thermodynamic parameters and binding energy for the binding processes.

Scope of the research

1. Study the binding interaction between quinoline derivatives with protein by spectroscopic methods.
2. Study the thermodynamic parameters by spectroscopic and molecular docking.
3. Study the binding site and binding energy between proteins with quinoline derivatives by molecular docking.

CHAPTER II

THEORY AND LITERATURE REVIEWS

This study is an inspection of the interaction mechanism of quinoline derivatives with serum albumin to receive important information to be used with design and development quinoline derivatives as domain HIV-1 RT inhibitors. The interactions system was investigated using the calculation method and experiment of binding parameters by UV- VIS spectroscopy, Fluorescence spectroscopy, and computational chemistry. General information and related research on topics are listed as follows.

Amino acids

Proteins

UV-VIS spectroscopy

Fluorescence spectroscopy

Thermodynamic parameters and binding model

Computational chemistry

Related research

Amino acids

Amino acids are organic compounds comprising NH₂, COOH group, a specific R Group for each amino acid and H atom. Proteins are made of amino acids linked by a peptide linkage. (Figure 4)

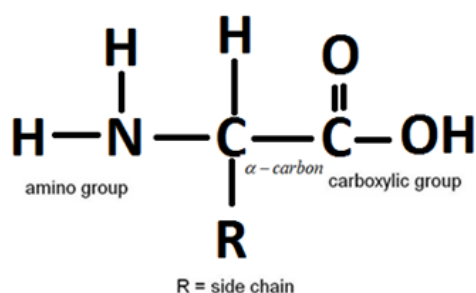


Figure 4 Basic structure of amino acid

Amino acids contain both COOH group and NH₂ group. Under specific pH conditions, a proton (H⁺) was carrying from the -NH₂ group to the -COOH group, leaving an ion with both a negative (-) and a positive charge (+), which is called a zwitterion (Figure 5).

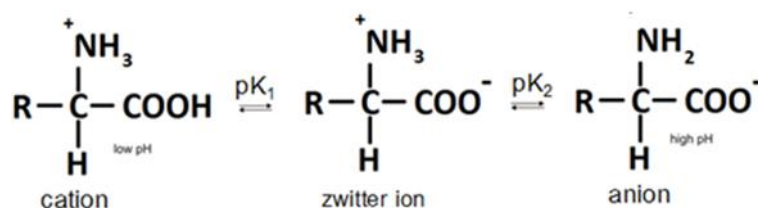


Figure 5 Zwitterion

There are 20 canonical amino acids most commonly found in nature. Each amino acids have a different side chain, which provides a unique role in protein structures and properties. Depend on the varieties of the R group, amino acids can be divided into 5 types.

Aromatic amino acids including phenylalanine, tyrosine, and tryptophan (Figure 6). These amino acids can absorb radiation at near-ultraviolet light.

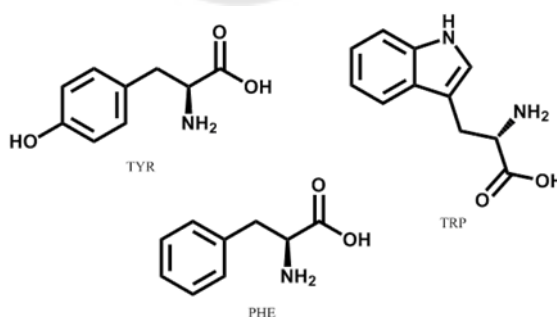


Figure 6 Aromatic amino acids

Polar amino acids uncharged such as serine (Ser), cysteine (Cys), threonine (The), glutamine (Gln), and asparagine (Asn). These amino acids are relatively hydrophilic (water-loving) (Figure 7).

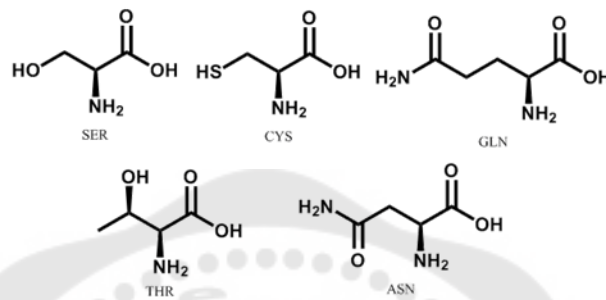


Figure 7 Polar uncharged amino acids

Nonpolar amino acids such as leucine (Leu), alanine (Ala), valine (Val), proline (Pro), isoleucine (Ile), glycine (Gly), and methionine (Met) (Figure 8). These amino acids are hydrophobic and thus face the inside of protein structures.

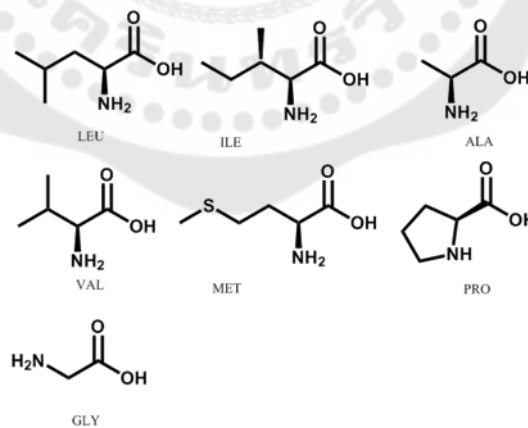


Figure 8 Nonpolar amino acids

Positive charged amino acids such as histidine (His), lysine (Lys) and arginine (Arg) (Figure 9).

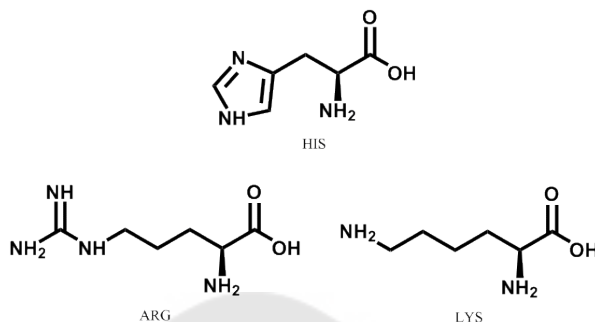


Figure 9 Positive charged amino acids

Negative charged amino acids: aspartic acid (Asp) and glutamic acid (Glu) (Figure 10).

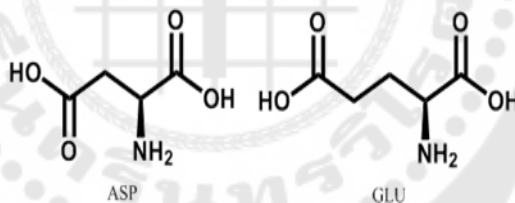


Figure 10 Negative charged amino acids

Peptides are biopolymers containing a sequence of amino acids. Each amino acid is bound together by a covalent bond. Which is called as a peptide bond. The NH₂ group of another amino acid blends a single amino acid with the COOH group, causing an amide bond and leaving a molecule of water. The resulting amide bond is called the peptide bond and the matters formed by this linkage are peptides (Figure 11).

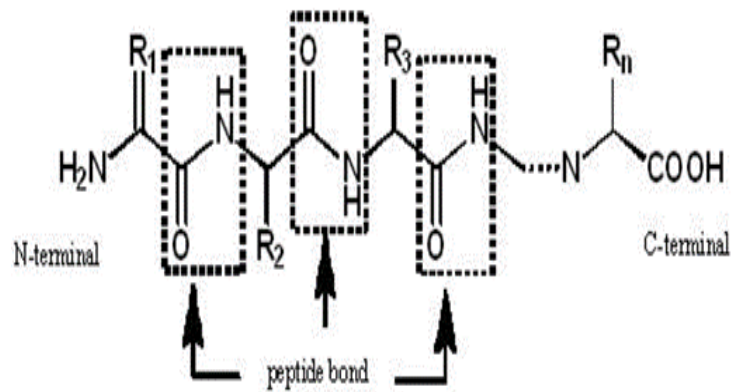


Figure 11 Peptide bond of amino acids

Proteins

Proteins made of amino acids more than 10 kDa. The structure is more complex than the peptide chains and can be divided into 4 structures as shown in Figure 12 (Russell, 2010).

Primary structure

The primary structure is the fundamental structure of all amino acid proteins that have a definite sequence that continues with the peptide bond.

Secondary structure

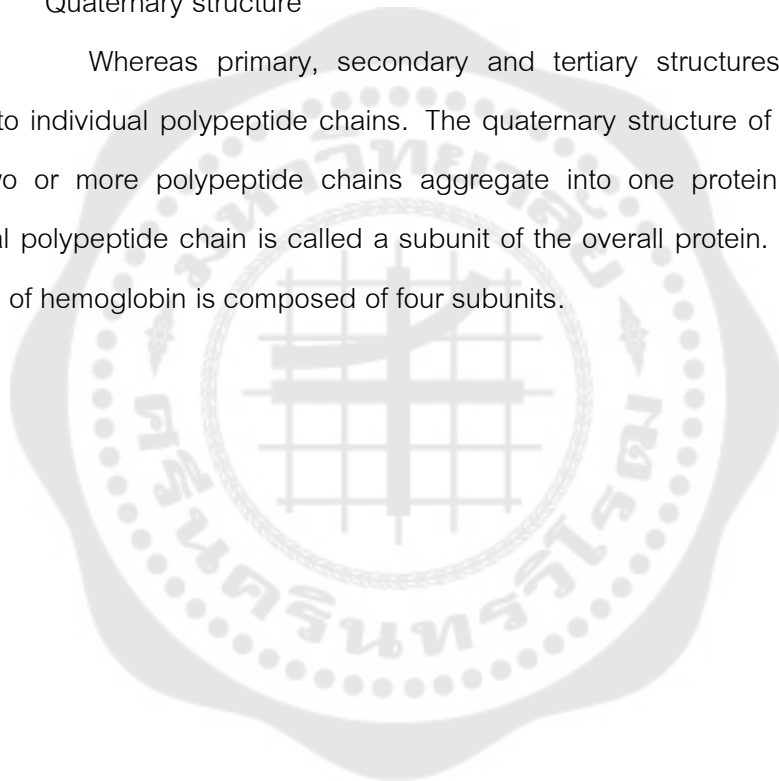
In certain regions the polypeptide chain can be folded, providing the protein's secondary structure. The most commonly found secondary structures are the α -helix and β -pleated sheet. The α -helix is a coiled strand with the right-hand side. The side chains substituents of the NH₂ groups in an α -helix are spread outwards. The oxygen of carbonyl (C=O) group and the amine H (N-H) of each peptide can form H bonding which is stabilizing the bond between the peptide strand. The H bonding in a β -sheet has two different types; between inter-strand and within intra-strand. The β -sheet conformation involves pairs of strands side by side. The amino Hs in a single strand H bond with the contiguous strand carbonyl oxygen.

Tertiary structure

The three-dimensional structure of the entire polypeptide chain is called tertiary structure. The electrostatic interaction between polar functional groups such as carboxylate ($-\text{COO}^-$) and ammonium salt ($-\text{NH}_3^+$) can stabilize the tertiary structure of proteins. The chemical interactions like disulfide bonding can also stabilize the protein tertiary structure. Specifically, this kind of interaction occurs among R groups containing sulfur atom such as Cys and Met.

Quaternary structure

Whereas primary, secondary and tertiary structures of proteins are applied to individual polypeptide chains. The quaternary structure of proteins is adopted when two or more polypeptide chains aggregate into one protein complex. Each individual polypeptide chain is called a subunit of the overall protein. For example, the structure of hemoglobin is composed of four subunits.



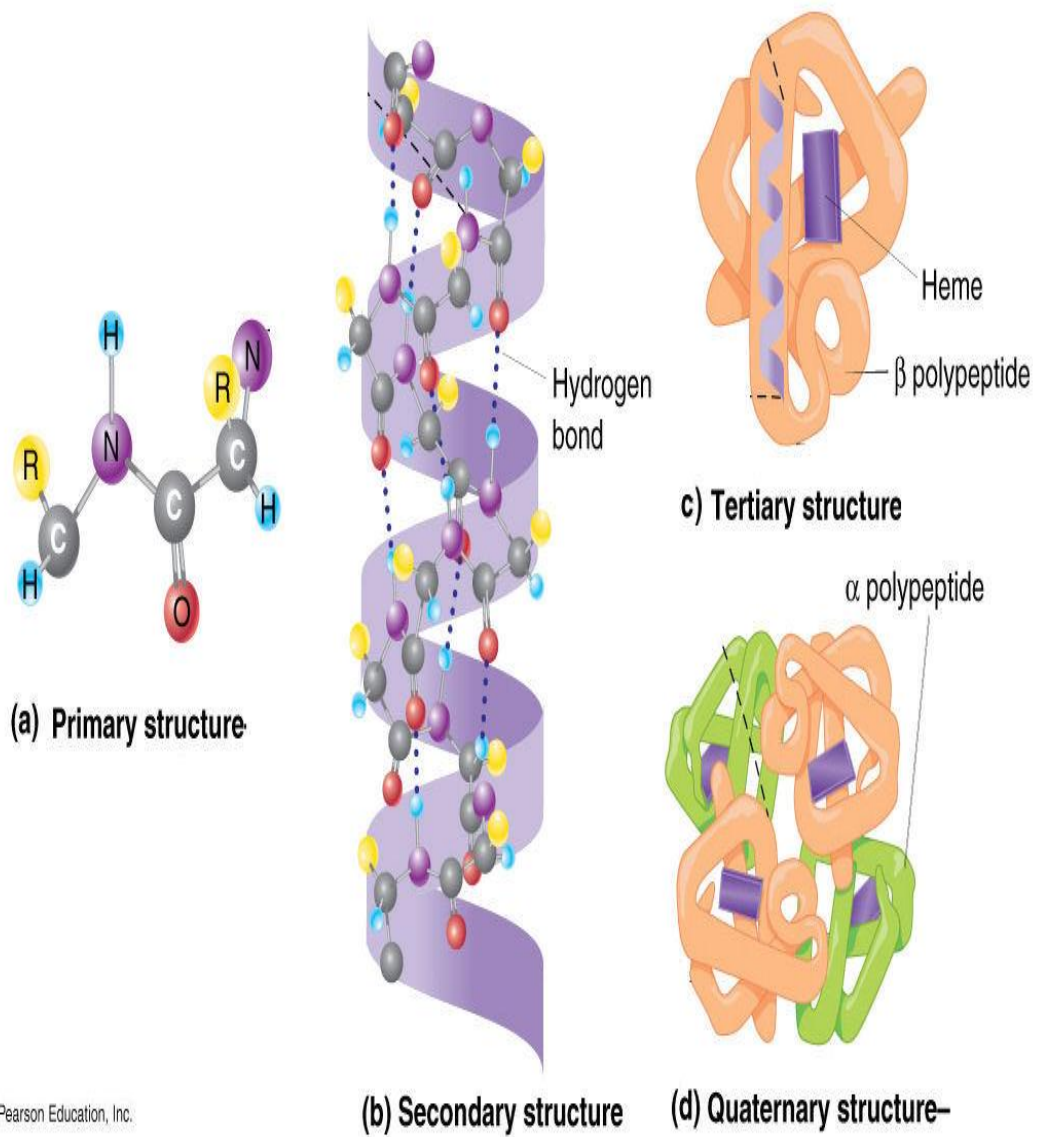


Figure 12 Four structures of proteins

Source: Russell, P. (2010). *iGenetics* (3 ed.): Steven M. Carr.

UV-VIS spectroscopy

UV- VIS radiations consist of only a diminutive part of the spectrum of electromagnetic in the frequency range of 10^{14} - 10^{18} Hz., as shown in Figure 13 (Owen, 1996).

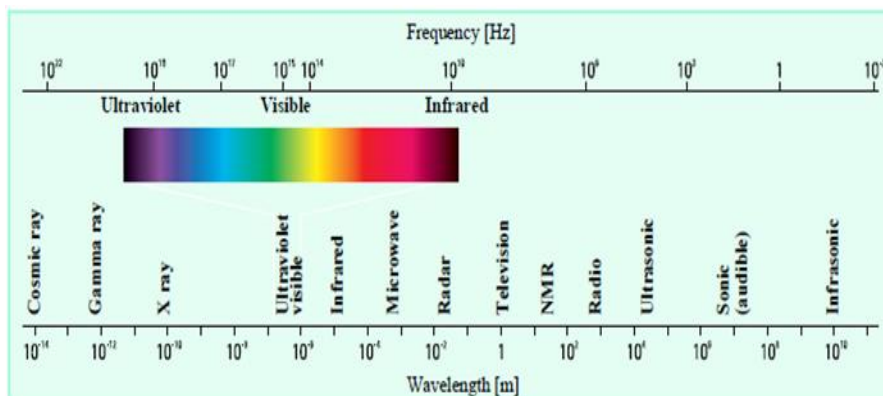


Figure 13 Schematic diagram of electromagnetic spectrum

Source: Owen, T. (1996). Fundamentals of Modern UV-Visible Spectroscopy :
A Primer: Hewlett-Packard

The energy of electromagnetic radiation was associated with is determined by equation 1 as shown:

$$E = h\nu \quad \text{---- [1]}$$

E is energy

h is Planck's constant (6.62×10^{-34} Js)

ν is frequency (s^{-1})

Electromagnetic wave radiation can be said to be a combination of a diverse magnetic and electric field that travels perpendicularly thru space with wave movement. Since radiation acts as a wave, it can be classified in a system of wavelengths or frequencies, which are correlated to the equation as shown:

$$\nu = \frac{c}{\lambda} \quad \text{---- [2]}$$

c is the speed of light ($3 \times 10^8 \text{ ms}^{-1}$)

λ is wavelength (nm)

UV-VIS radiations interact with a matter which causes electronic transitions. The transition in molecular electronics happens when the electrons in the molecule are excited from low energy to higher energy state. The changes in energy associated with this change provide data on the molecular structure and determine many characteristics of the molecular structure. (Figure 14).

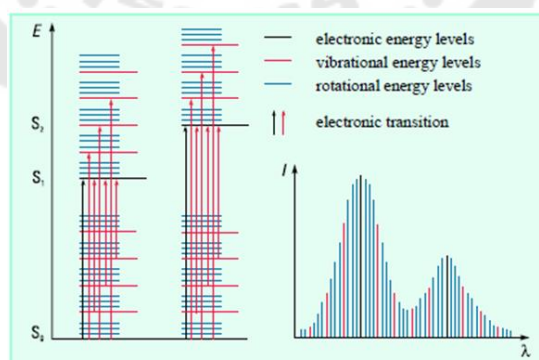


Figure 14 The electronic transition

Source: Owen, T. (1996). Fundamentals of Modern UV-Visible Spectroscopy :
A Primer: Hewlett-Packard

UV / VIS spectrophotometer is a tool used to determine the amount of light and intensity in the range of UV and white light penetration or absorption. The wavelength of the light is related to the amount and type of substance in the sample, most of which are the substances that can absorb light at these wavelengths.

When the sample molecules are exposed to light in a range of ultraviolet or ultraviolet light. The electrons inside the atom absorb the light and change the state to a higher state of energy. When determining the amount of light passing or reflecting from a sample, relative to light from a source at the specific wavelength, the absorbance can be calculated according to the Beer-Lambert law as shown in equation 3.

$$A = \epsilon bc \quad \text{---- [3]}$$

A is the absorbance

ϵ is the molar absorption coefficient ($M^{-1} \text{ cm}^{-1}$)

b is the path length (cm)

C is the analyze concentration (M)

This technique can be used to study binding interactions between ligands with protein due to aromatic amino acids that are competent to absorb UV Ia in the UV region. The UV region ranged between 200-380 nm, while the VIS region ranged between 400-750 nm as shown in Figure 15. (Jr. et al., 2002).

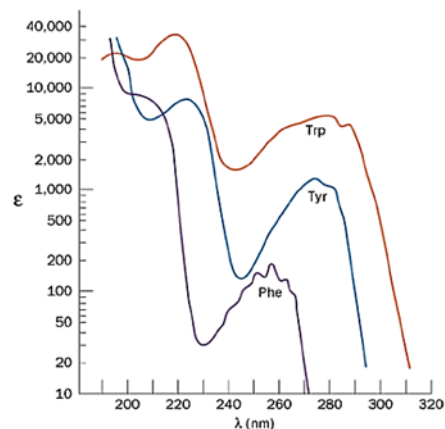


Figure 15 The absorption spectrum of aromatic amino acids

Source: Jr., I. T., Sauer, K., Wang, J. C., Puglisi, J. D., Harbison, G., & Rovnyak, D. (2002). *Physical Chemistry: Principles and Applications in Biological Sciences* (4 ed.). New Jersey: Prentice Hall, inc.

From the above spectra, tryptophan absorbs lighter than tyrosine and phenylalanine. Therefore, Trp is reciprocating for most of the absorbance of UV light (280 nm) by proteins.

Fluorescence spectroscopy

Fluorescence Emission spectroscopy is a method to be accustomed to analyzing the properties of a substance that can emit photons when the electrons are transferred back to the ground from the exciting stage (S_0). This emission occurs after the molecule absorbs UV radiation that causes the molecules to be excited to higher energy state. The molecules at higher energy state are unstable. Therefore, they release extra energy and fall into a lower energy level. Molecular energy is left from the first class of energy to the ground state, begetting the fluorescence emission of photons to form the emission spectrum at precise energies of the substance as shown in Figure 16 (Lleres, Swift, & Lamond, 2007).

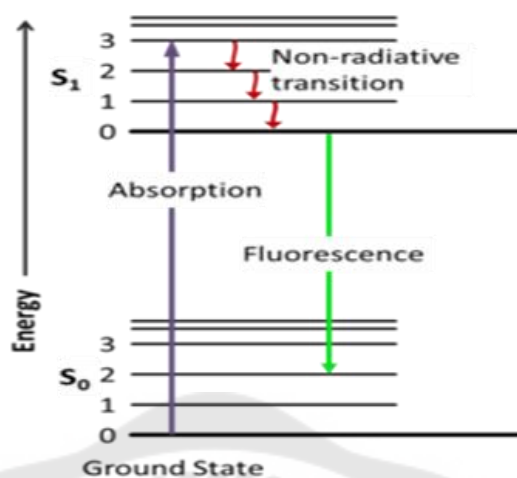


Figure 16 The transitions between electronic states of a molecule

Source: Lleres, D., Swift, S., & Lamond, A. I. (2007). Detecting protein-protein interactions in vivo with FRET using multiphoton fluorescence lifetime imaging microscopy (FLIM). *Curr Protoc Cytom, Chapter 12, Unit12 10*.

Residues of Phe, Tyr, and Trp can emit fluorescent radiation from proteins. Trp has the most intense fluorescence and is sensitive to changes in the protein's surroundings. Therefore, TRP is commonly used as a fluorescent probe to examine drug-protein binding interactions. Moreover, mechanisms of the binding interaction between ligands and protein can be studied by fluorescence quenching methods.

The fluorescence quenching mechanisms

The serum albumin fluorescent quenching process pandered by drugs can be divided into static quenching and dynamic quenching. Static quenching as the higher temperature causes the complex structure less stable and the quenching constant decreases with the rise in temperature. In contrast, for dynamic quenching depends mostly on molecular collisions, if the higher temperature is the greater the diffusion coefficient, and the increase in temperature the quenching constant increases. Therefore,

The protein-quenching fluorescence mechanism depends on the temperature and the lifetime of the excited state as shown in Figure 17. (Seery et al., 2005, pp. 3426 – 3433).

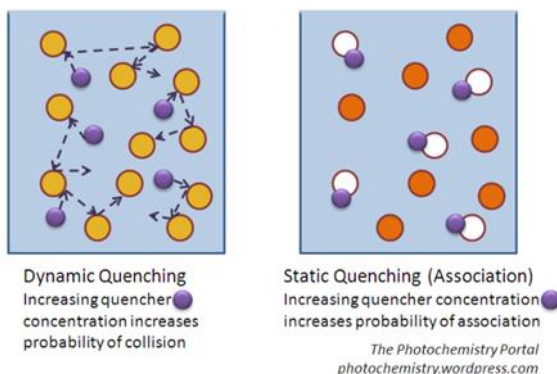


Figure 17 the quenching mechanism

Source: Seery, M., Fay, N., McCormac, T., Dempsey, E., Forster, R., & Keyes, T. (2005). Photophysics of Ruthenium Polypyridyl Complexes formed with lacunary polyoxotungstates with iron addenda. *Physical Chemistry Chemical Physics*, 19(7), 3426 – 3433.

In this work, the fluorescence quenching can be classified as static quenching or dynamic quenching between serum albumin and quinoline derivatives. This can be established by experiments that quench fluorescence at three different temperatures. The constant of fluorescence quenching can be evaluated by using the Stern–Volmer equation (equation 4).

$$\frac{F_0}{F} = 1 + K_{sv}[Q] = 1 + K_q\tau_0 \quad \text{---- [4]}$$

F_0 is the fluorescence intensity in the absence of quencher

F is the fluorescence intensity in the presence of quencher

K_{sv} is the Stern-Volmer quenching constant

K_q is the quenching rate constant

τ_0 is the fluorescence lifetime of protein without any quencher

$[Q]$ is the initial concentration of quencher

For the binding constant (K_b) and the number of binding sites (n) can be determined for the quenching mechanism between serum albumin with quinoline derivatives as shown in equation 5.

$$\frac{\log(F_0 - F)}{F} = \log K_b + n \log [Q] \quad \text{---- [5]}$$

K_b is the binding constant

n is the number of binding sites

Thermodynamic parameters and binding model

The ligand-protein binding mode, there are mostly 4 types of non-covalent interactions, as follows Van der Waals forces, H bonding interaction, electrostatic interaction, and hydrophobic interaction.

The signs of thermodynamic parameters such as entropy change (ΔS), enthalpy change (ΔH), and Gibbs free energy (ΔG) in protein binding mode can be used to approve the binding model. Normally, it is suggested that both entropy change (ΔS) and enthalpy change (ΔH) were negative, indicating that Vander Waals force or H bonding interaction was the interaction force. Entropy change (ΔS), the enthalpy change (ΔH) are positive, indicating that the interaction force was a hydrophobic interaction. The change

in enthalpy (ΔH) is almost zero and the change in entropy (ΔS) is positive, suggesting that the interaction force was electrostatic. The Van't Hoff equations can decide the thermodynamic parameters in the binding model between protein and ligand as shown in equations 6, 7. (Ross & Subramanian, 1981a, pp. 3096-3102)

$$\Delta G = -RT \ln K_b \quad \text{---- [6]}$$

$$\ln K_b = -\frac{\Delta H}{RT} + \Delta S/R \quad \text{---- [7]}$$

ΔG is Gibbs free energy changes

ΔH is enthalpy changes

ΔS is entropy changes

T is a temperature

R is a gas constant

The binding site of ligand on BSA and HAS

Many research reveals that small-molecule normally binds in subdomains IIA and IIIA of serum albumin inside two hydrophobic pockets. That is called site I and site II. Thus, the ligand-binding site on serum albumin can be identified through competitive binding experiments with drugs that specifically bind to a known serum albumin site. Warfarin is binding to sub-domain IIA while ibuprofen is binding to sub-domain IIIA. The binding site between ligand on serum albumin can be determined by the fluorescence competitive binding experiments as shown in Figure 18. (Khodarahmi et al., 2012).

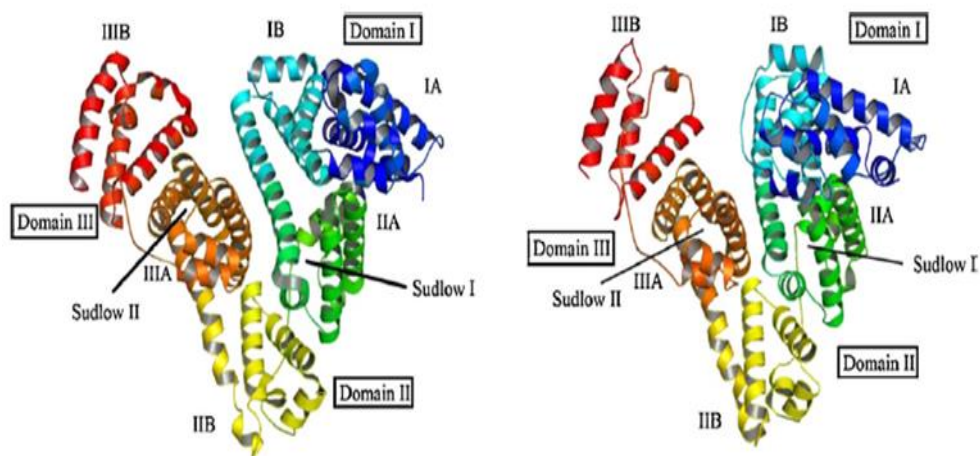


Figure 18 The locations of domain-binding sites of HSA (left) and BSA (right)

Source: Khodarahmi, R., Karimi, S. A., Ashrafi Kooshk, M. R., Ghadami, S. A., Ghobadi, S., & Amani, M. (2012). Comparative spectroscopic studies on drug binding characteristics and protein surface hydrophobicity of native and modified forms of bovine serum albumin: possible relevance to change in protein structure/function upon non-enzymatic glycation. *Spectrochim Acta A Mol Biomol Spectrosc*, 89, 177-186.

Computational chemistry

Computational chemistry is the use of computer calculations to solve chemical problems, which uses methods of theoretical chemistry, included in the powerful computer program for calculating the structure and properties of molecules. We used molecular docking in this work to study the binding relationship between ligand and protein to obtain binding sites and binding energy.

Molecular docking

Molecular docking predicts that both molecules will interact, which is explained by the binding energy and the binding site of the 3D structure of the ligand-protein complex. The ligand-receptor binding mechanism is the lock and key theory. The interaction of ligand-receptor suggests that the ligand and the receptor possess specific complementary geometric shapes that fit exactly into one another as shown in Figure 19. Molecular docking is an important element in drug discovery and design. This method has been used

consistently and successfully in pharmaceutical and medical research. Molecular docking can be used to study small ligand 's binding position on the protein, which also results in the binding position on the protein binding site and binding energy. (Wei, Weaver, Ferrari, Matthews, & Shoichet, 2004-1182).

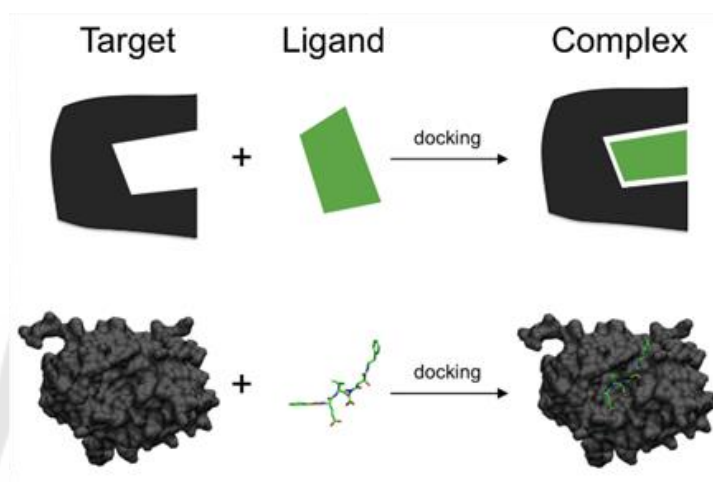


Figure 19 The lock and key theory

Source: Wei, B. Q., Weaver, L. H., Ferrari, A. M., Matthews, B. W., & Shoichet, B. K. (2004). Testing a flexible-receptor docking algorithm in a model binding site. *J Mol Biol*, 337(5), 1161-1182.

Molecular docking can be divided into 2 methods, docking and reverse docking methods. In the reverse docking method, a small ligand of interest is docked into the binding site of various protein structures, which can be downloaded from the protein database to obtain a suitable protein. On the other hand, in the docking method, a protein of interest is docked into various small ligand structures, downloaded from the chemical database, to obtain a suitable ligand. The comparison of these two paradigms is shown in Figure 20. (Zheng et al., 2013, pp. 549-559).

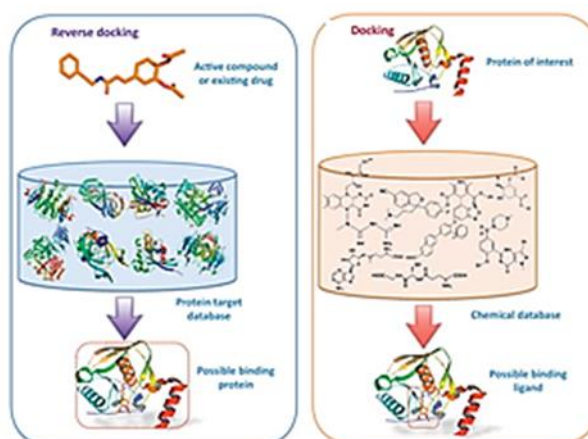


Figure 20 Comparison of docking and reverse docking.

Source: Zheng, M. , Liu, X. , Xu, Y. , Li, H. , Luo, C. , & Jiang, H. (2013). Computational methods for drug design and discovery: focus on China. *Trends Pharmacol Sci*, 34(10), 549-559.

Related research

Many studies have demonstrated the properties and characteristics of quinoline derivatives for numbers of pharmacological and biological activities, such as anti-HIV antimalarial activity, anti-inflammatory activity, antibacterial, analgesic activity, antineoplastic, antifungal, and antiviral.

Antimalarial activity

In 1996, Raynes and coworkers (Raynes, Foley, Tilley, & Deady, 1996, pp. 551- 559) synthesized bisquinoline compounds and found that these compounds possessed a good activity of antimalarial action to inhibit both chloroquine-sensitive parasites of *Plasmodium falciparum* and chloroquine-resistant (Figure 21).

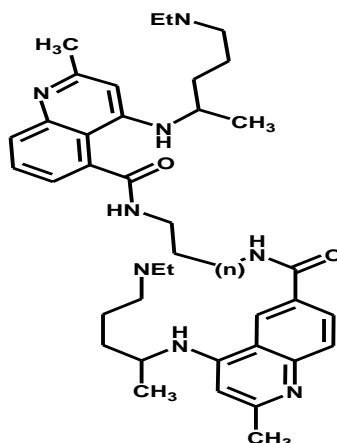


Figure 21 Bisquinoline compounds

In 2009, Modapa and coworkers (Madapa et al., 2009, pp. 203-211) investigated 2-methyl-6-ureido-4-quinolinamides for their antimalarial activity. This represents the antimalarial effect of a compound at a minimum inhibitory concentration of 0.35 mg/mL inhibit chloroquine-sensitive of *Plasmodium falciparum* strain. The compounds showed a good percent antibacterial effect inhibits bacteria with many-fold greater than the drug gentamicin (Figure 22).

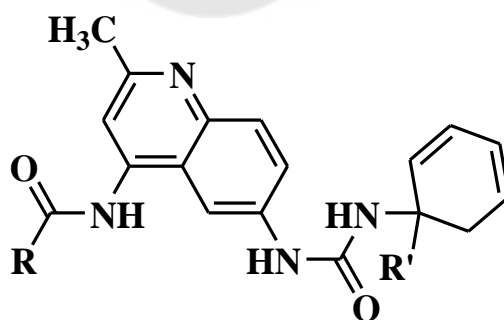


Figure 22 2-methyl-6-ureido-4-quinolinamides

Anti-inflammatory activity

In 1996, Baba and coworkers (Baba et al., 1996, pp. 5176-5182) developed and synthesized quinolone derivative ethyl : 4-(3,4-dimethoxyphenyl)-6,7-dimethoxy-2-(1,2,4-triazol-1-yl-methyl) quinolone-3-carboxylate for disease-modifying antirheumatic drugs (DMARDs). These compounds were tested for anti-inflammatory effects by using the AA rat model. The result showed that quinolone derivative having a median effective dose value of 2.8 mg/kg/day in the AA rat which is considered to be medicine for future investigations. (Figure 23).

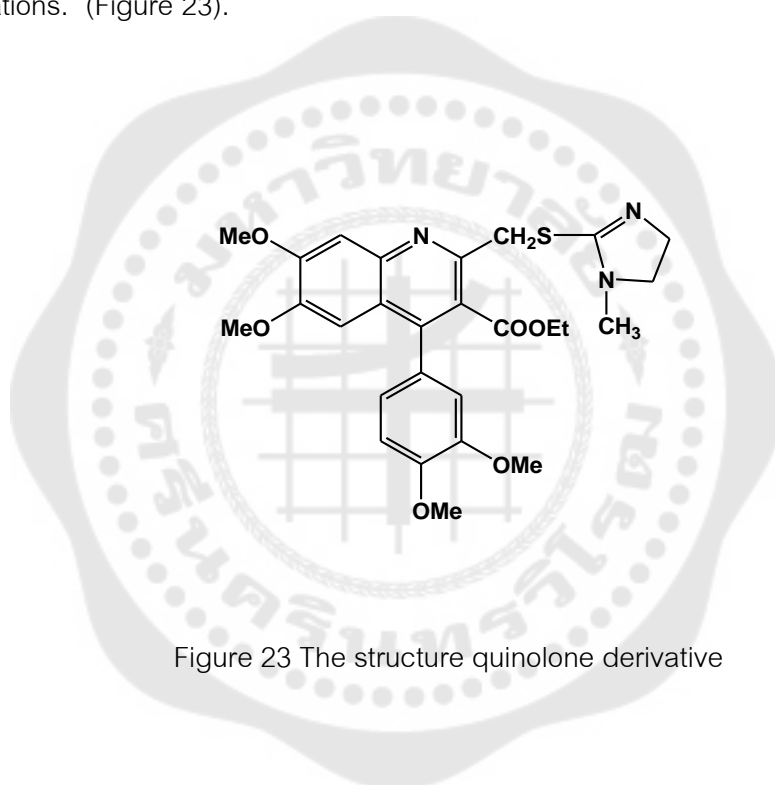


Figure 23 The structure quinolone derivative

Antibacterial

In 2009, Upadhyaya and coworkers (Upadhyaya et al., 2009, pp. 2830-2841) designed and synthesized quinoline derivative to study for biological evaluation and molecular docking against *Mycobacterium tuberculosis*. This quinolone derivative showed antibacterial effect at MIC of 6.27 $\mu\text{g/mL}$ inhibit *Mycobacterium tuberculosis* and the binding process was electrostatic interaction (Figure 24).

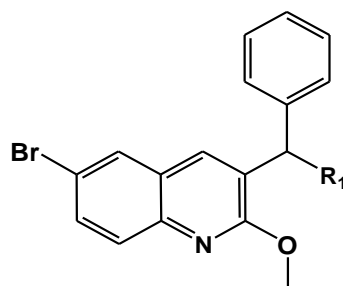
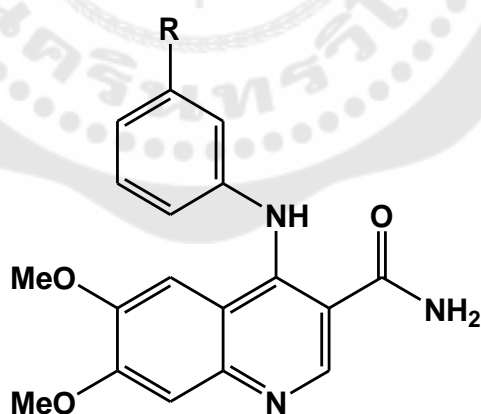


Figure 24 3-benzyl-6-bromo-2-methoxy-quinolines

Antineoplastic

In 2009, Scott and coworkers (Scott et al., 2009, pp. 697-700) have developed 3-amido-4-anilinoquinolines which have been found to have a good antitumor by inhibiting CSF-1R kinase. The results showed that 3-amido-4-anilinoquinolines were good effective CSF-1R inhibitors with great selectivity of kinase and good activity in mouse PD, and they can display activities in a rat model with 3-amido-4-anilinoquinolines (Figure 25).

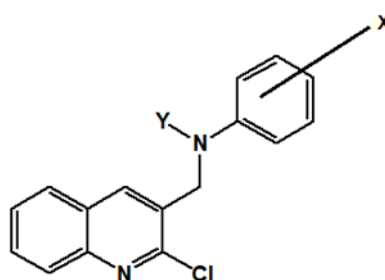


R = F, Cl, Br, CH₃

Figure 25 3-Amido-4-anilinoquinolines

Antifungal

In 2011, Kumar and coworkers (Kumar, Bawa, Drabu, & Panda, 2010, pp. 6705-6715) were designed and synthesized 2-chloroquinoline derivatives as antifungal agents. The results showed that 2-chloroquinoline had antifungal activity inhibit *Aspergillus niger*, *A. flavus*, *Penicillium*, and *Monascus purpureus* (Figure 26).



X = F, Cl, Br, CH₃, NO₂, Dichloro ; Y = H, CH₃

Figure 26 2-chloroquinoline derivatives

Antiviral

In 2008, Ghosh and coworkers (Ghosh et al., 2008, pp. 349-353) were synthesized 2-(2-methyl-quinoline-4ylamino)-N-(2-chlorophenyl)-acetamide for neuroprotection inhibitors and Japanese encephalitis. They were found to have a good percent of antiviral action inhibit the Japanese encephalitis virus (Figure 27).

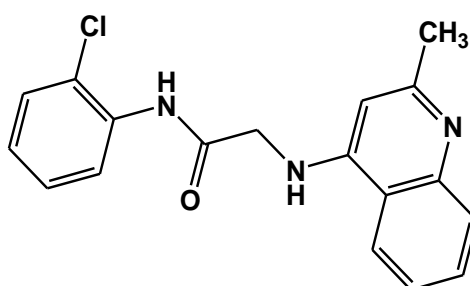


Figure 27 Anilidoquinoline derivative

Anti-HIV

In 2009, Da Silva and coworkers (Da Silva Fde et al., 2009, pp. 373-383) synthesized 1-benzyl-1H-1,2,3-Triazole derivatives seen on various carbohydrate systems and inhibitory profiles in vitro inhibit HIV-1 RT. The data found that 2a and 2d as the most active compounds found that potent activity of the HIV-1 RT catalytic with cytotoxicity lower than Zidovudine and greater than zalcitabine and didanosine (Figure 28).

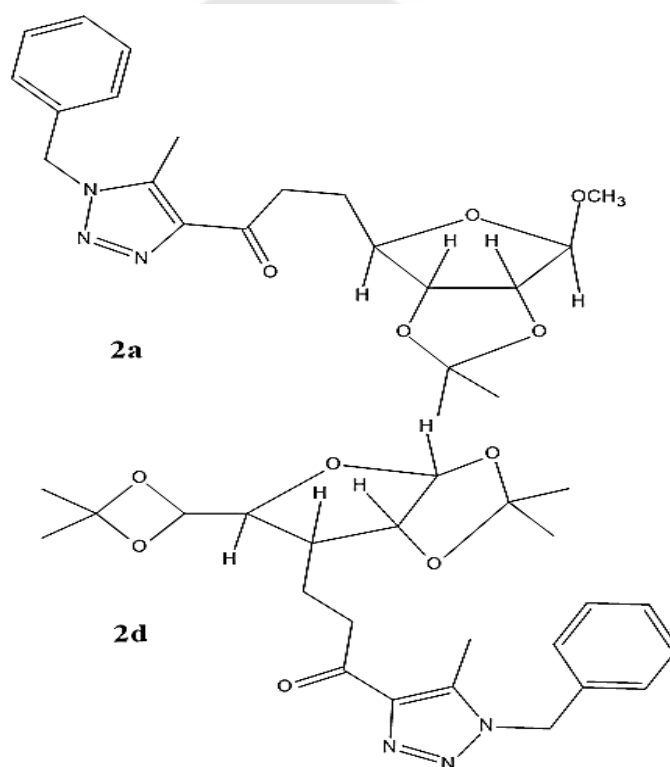


Figure 28 1-benzyl-1H-1,2,3-triazole derivatives

In 2012, Ashchop and coworkers (Asahchop, Wainberg, Sloan, & Tremblay, 2012, pp. 5000-5008) studied drug resistance for anti HIV-1 RT and developed of new HIV-1 RT inhibitors. The results found that an ideal new HIV inhibitor should have a high

genetic barrier in terms of developing resistance to the same type of drug. -1 RT (Figure 29).

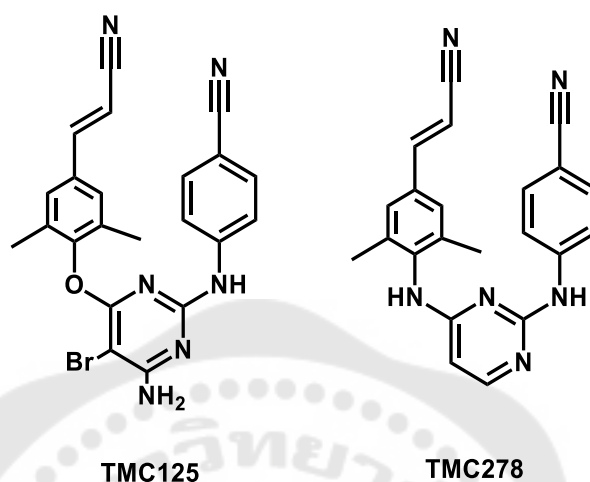


Figure 29 The new HIV-1 reverse transcriptase inhibitors

In 2013, Mathes and coworkers studied effective evaluation of increases in duration of first HAART over time (1996-2009) and associated factors in the multicenter AIDS cohort study. The results showed that 1009 participants, 796 changed regulation within 5.5 years after HAART initiation. The improved HIV suppressive efficacy and increased convenience of newer regimens as evidenced by progressive reductions over time in the mean the number of pills received in initial HAART regimens, indicate that current HIV treatment optimizes the likelihood of extended first HAART durability and improved patient quality of life.

In 2013, Tremblay and coworkers (Tremblay et al., 2013, pp. 2775-2780) researched and tested benzofurano[3,2-d] pyrimidin-2-one derivatives for RT-competent HIV-1 nucleotide agents. The results found that the compounds were demonstrated potential inhibit the virus resistant to HIV-1 RT. (Figure 30).

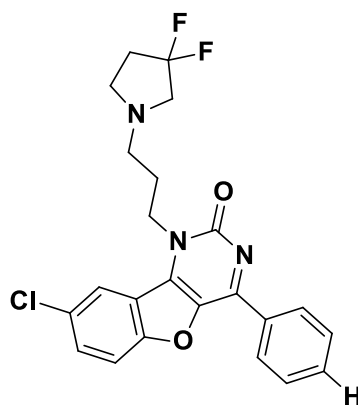


Figure 30 benzofurano[3,2-d]pyrimidin-2-ones

In 2017, Chander and coworkers (Chander et al., 2017, pp. 74-79) designed, synthesized, and characterized 5- benzoyl- 4- methyl- 1,3,4,5- tetrahydro- 2H- 1,5- benzodiazepin-2-one derivatives for anti-HIV-1 RT agent. The results showed that in-vitro enzyme-screened derivatives inhibit wild HIV-1 RT with Enzyme-linked Immunosorbent Assay. The findings showed that four compounds with a half- maximal inhibitory concentration ≤ 26 mM were strongly opposed to the Reverse Transcriptase activity. Furthermore, In the in-vitro assay, three significantly active compounds of the sequence, A1 and A10, showed half the maximum inhibitory concentration values of 8,64 and 6,96 mM respectively. (Figure 31).

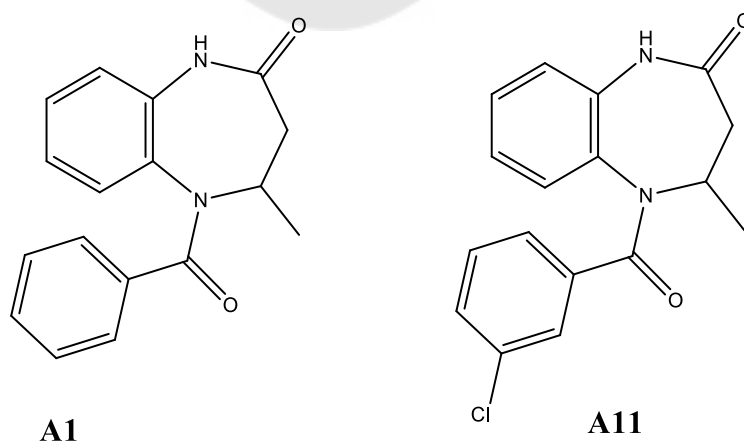


Figure 31 the compounds A1 and A11

In 2019, Makarasen and coworkers (Makarasen et al., 2019, pp. 671-682) designed amino-oxydiarylquinoline derivatives by molecular docking methods after that these derivatives are synthesized as activity non-nucleoside HIV-1 RT agents. The results showed that 7a and 7d were the most anti-HIV-RT inhibitors among the compounds designed, developed and synthesized, and the inhibition rates at 2 μM were 35.0 percent and 38.7 percent. (Figure 32).

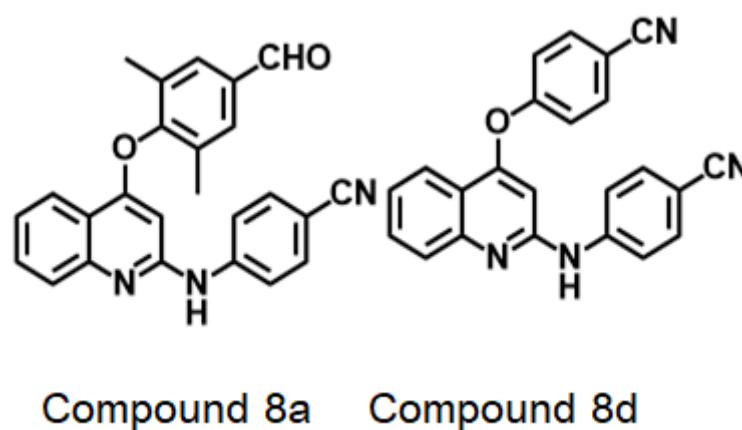


Figure 32 Amino-oxydiarylquinoline Derivatives

The binding interaction between molecules of drug with BSA and HSA was importance and basic necessity. It is of interest to researchers in the applied life sciences, chemistry, and medicine.

In 2013, Sarkar and coworkers (Sarkar, Paul, & Mukherjea, 2013, pp. 220-230) studied alprazolam's binding interaction with BSA using physicochemical, photophysical, and molecular docking methods. The results indicated that the quenching mechanism between BSA and alprazolam has been a static quenching mechanism with a strong binding constant and a binding site number of 1. Alprazolam was spontaneous bind to BSA in the site I, and interaction forces were hydrophobic forces (Figure 33).

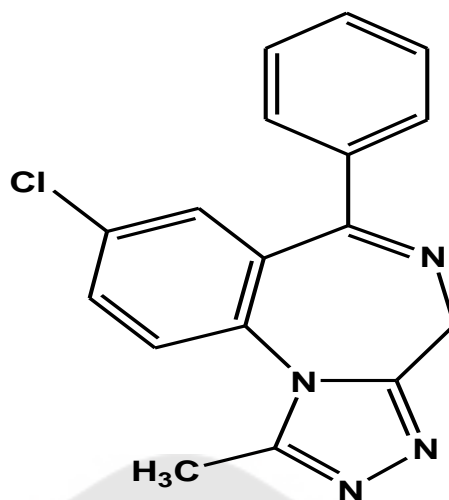


Figure 33 Alprazolam

In the same year, Shahabadi and coworkers (Shahabadi, Khorshidi, & Moghadam, 2013, pp. 627-632) studied the binding relationship between zonisamide, using spectroscopy and molecular docking methods with human serum albumin (HSA). The results showed that the fluorescence quenching mechanism between zonisamide HSA was a static quenching process and binding site number was 1. Zonisamide was spontaneous bind to HSA in subdomain IIA, and the interaction force was H bonds and hydrophobic interaction (Figure 34).

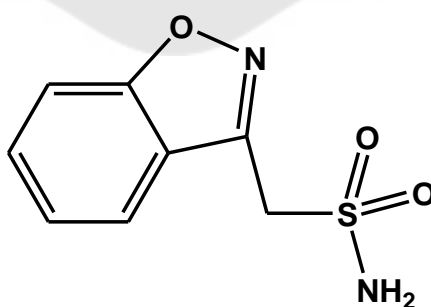


Figure 34 Zonisamide

In 2017, Xu and coworkers (Xu et al., 2017, pp. 174-178) have studied tussilagone binding mechanisms with HSA using fluorescence spectroscopy and molecular docking methods. The results showed that a static quenching mechanism between HSA and tussilagone. The binding constant (K_b) between HSA and tussilagone was $2.182 \times 10^3 \text{ L mol}^{-1}$ and the binding site number was 1. Tussilagone was spontaneous bind to HSA in subdomain IIA, and interaction forces were hydrophobic forces and H bonds (Figure 35).

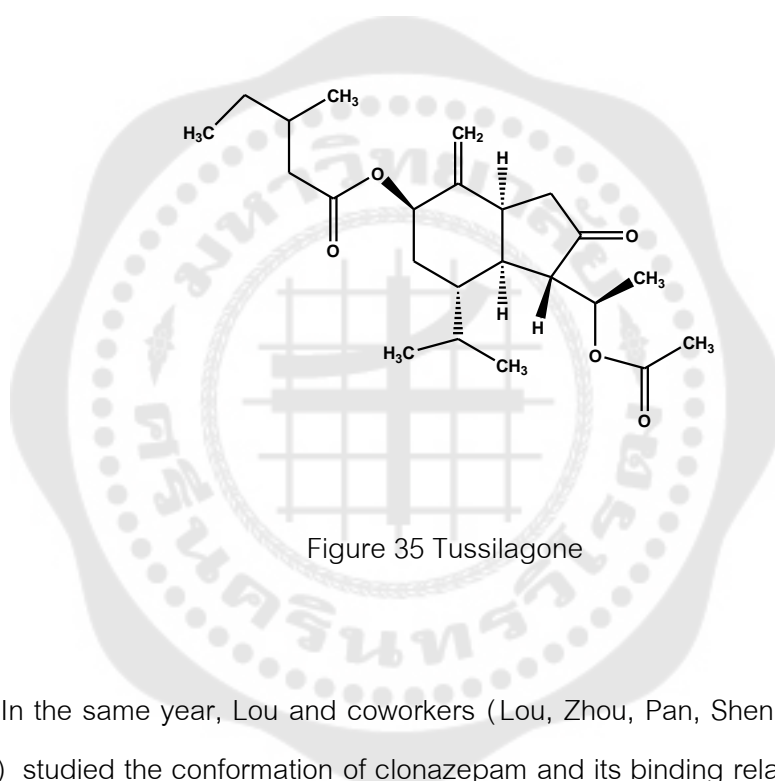


Figure 35 Tussilagone

In the same year, Lou and coworkers (Lou, Zhou, Pan, Shen, & Shi, 2017, pp. 158-167) studied the conformation of clonazepam and its binding relationship with BSA using spectroscopy and molecular docking techniques. The results showed that the static quenching process between BSA and clonazepam. The binding constant (K_b) between BSA with clonazepam molecule was $7.94 \times 10^4 \text{ L mol}^{-1}$ and the binding site number was 1. clonazepam was spontaneous bind to BSA in subdomain IIA, and interaction forces were hydrophobic forces and H bonds (Figure 36).

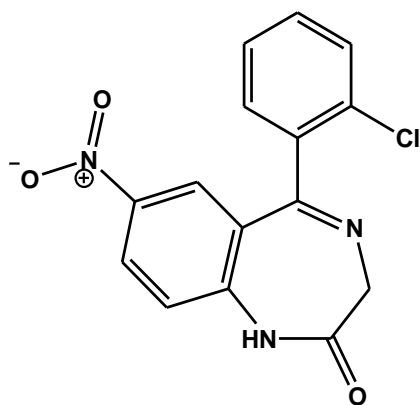


Figure 36 Clonazepam



CHAPTER III

EXPERIMENTAL

Equipment

Precision analytical balance digital scale, Mettler Toledo, code AB104-S

Micropipette (2, 10, 20, 100, 200 and 1000 mL), Gilson

pH meter, Mettler Toledo

Cavitator ultrasonic cleaner, Mettler Electronics Corp

UV-VIS spectrophotometer, Shimadza, code UV-2401 PC

Fluorescence spectrophotometer, Jasco, code FP-6200 PC

Chemical reagents

4-(4'-cyanophenoxy)-2-(4''-cyanophenyl)-aminoquinoline (1), Chulabhorn
Research Institute

4-(4'-cyanophenoxy)-2-(5''-cyanopyridinyl)-aminoquinoline (2), Chulabhorn
Research Institute

Hydrochloric acid (HCl), QReC™ Quality Reagent Chemical

Trizma hydrochloride, Sigma-Aldrich

Sodium hydroxide, Carlo Erbra

Bovine serum albumin (BSA), Sigma-Aldrich

Human serum albumin (HSA), Sigma-Aldrich

Warfarin, Tokyo Chemical Industry

Ibuprofen, Tokyo Chemical Industry

Methods

UV spectra measurements

In the absence and presence of quinoline derivatives, UV spectra of both serum albumin solutions in 50 mM Tris-HCl buffer, pH 7.0 will be recorded on UV-spectrophotometer at room temperature from 250 to 500 nm. The concentration of serum albumin is 5 μM with increasing compound (1) and compound (2) concentration (10, 20, 30, 40, and 50 μM).

Fluorescence quenching measurements

The fluorescence spectrophotometer is used for the technique of fluorescence quenching mechanism. The excitation wavelength is set at 290 nm and the fluorescence emission spectra at different temperatures (299, 309, and 318 K) are estimated from 310 to 700 nm. The concentrations of serum albumin are set constant at 5 μM , while varying compound (1) and compound (2) concentration (2, 4, 6, 8, 10, 12 μM) in 50 mM Tris-HCl buffer, pH 7.0. The quinoline derivatives can determine the quenching constant of serum albumin by the Stern–Volmer equation (equation 4).

Binding constant and number of binding site

The binding constant and number of binding site (n) can be determined by the following equation 5 (chapter 2).

Thermodynamic parameters and binding model

For the thermodynamic parameters and binding model can be calculated by the Van't Hoff equation (equation 6, 7).

Competitive binding experiments

Competitive binding experiments of compound (1) and compound (2) on BSA and HAS. The experiments will be carried out using drugs included warfarin and ibuprofen as BSA and HSA site markers. Warfarin and ibuprofen are identified as markers for subdomain IIA site I and subdomain IIIA site II, respectively. The concentration of protein and site markers are set at 6 μM , while increasing quinoline derivatives concentration (2, 4, 6, 8, 10, 12 μM) in 50 mM Tris-HCl buffer, pH 7.0. The excitation wavelength is set at 290 nm, and at room temperature, the fluorescence emission spectra are measured at 310 to 700 nm.

Molecular docking

Molecular docking can be used to study the binding site and small ligand binding energy on the protein. The compound geometry was completely optimized by the functional density theory (DFT) at level B3LYP/6-31G(d, p) acquired in Gaussian 09. The BSA (4F5S) and HSA (1AO6) crystal structure are obtained from Protein Data Bank. The molecular docking using AutoDock 4.2 simulates the binding interactions between quinoline derivatives with serum albumin. The results of the Molecular docking can be explained by Accelrys Discovery Studio Client 4.0.

CHAPTER IV

RESULTS AND DISCUSSION

UV-Vis Spectra

UV-Vis spectroscopy has been used to investigate the ligand-protein binding interaction due to the protein's ability to absorb UV light through aromatic amino acids. The serum albumin displayed a strong absorption band at 285 nm, corresponding to the transformation of the amino acid aromatic residues from π - π^* . The changes of the absorption band were monitored to investigate the interaction between the protein with (1) and (2). The BSA and HSA absorption spectra at a constant concentration of 5 μM were measured in the range of 240 – 340 nm, with the concentration of the compound (1) or compound (2) of 10 to 50 μM in the Tris-HCl buffer of 50 mM at pH 7.0. A slight blue shift of the absorption band from 280 nm to 278 nm was observed, with hyperchromic of the serum albumin absorption at 285 nm. The excitation spectra of serum albumin are shown in Figures 37 and 38, respectively. The results indicated that compound (1) and compound (2) bound with serum albumin.

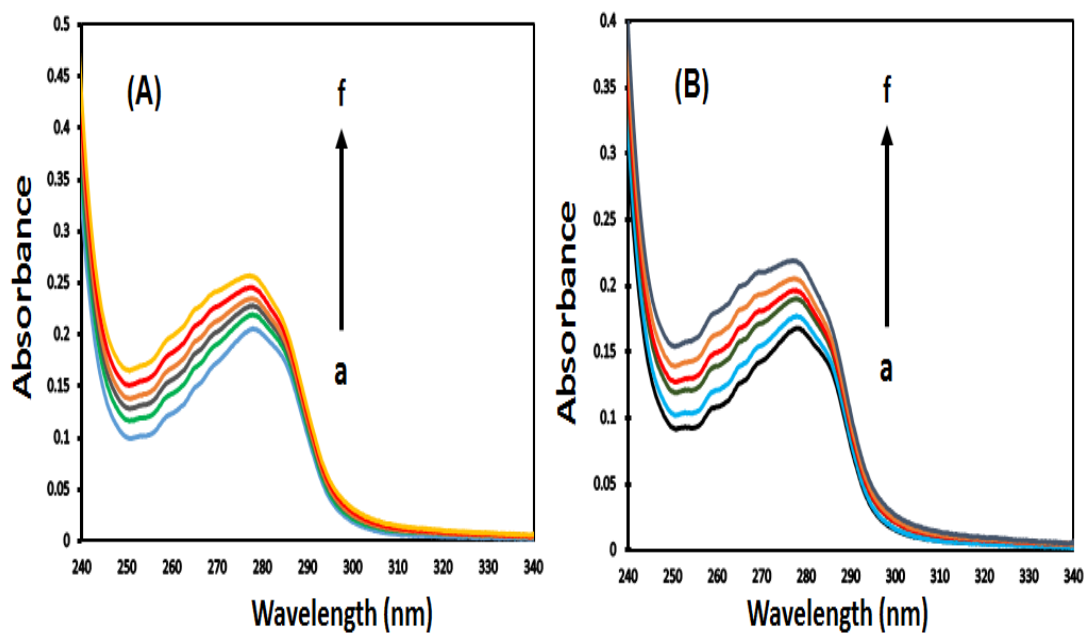


Figure 37 UV-VIS spectra of BSA (A) and HSA (B) with increasing the concentration of (1) (a-f). The concentration of serum albumin was kept at 6 μM with increasing the concentration of quinoline derivatives (1) (0, 10, 20, 30, 40, and 50 μM).

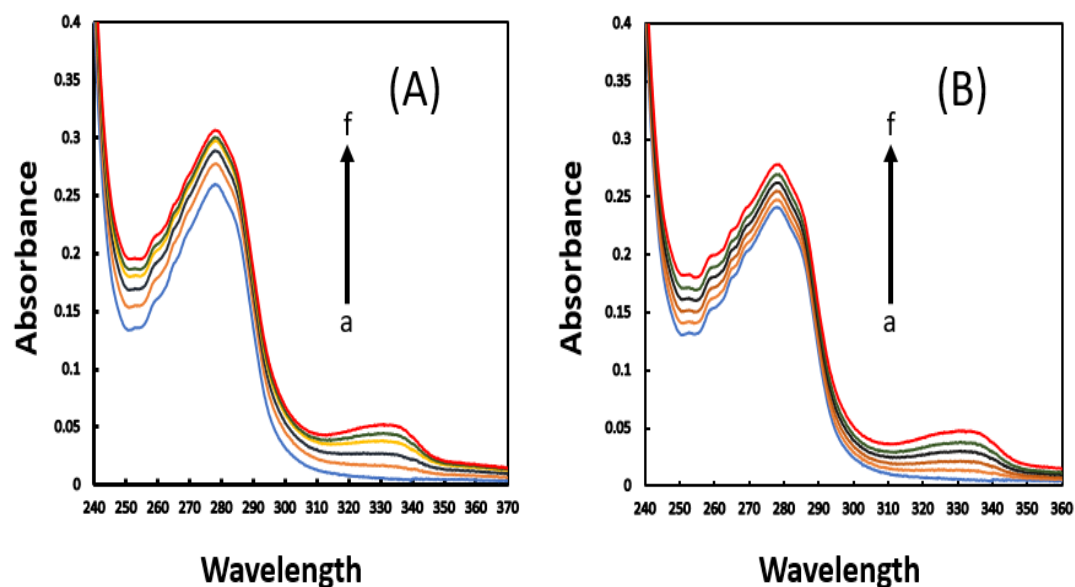


Figure 38 UV-VIS spectra of BSA (A) and HSA (B) with increasing the concentration of (2) (a-f). The concentration of serum albumin was kept at $5 \mu\text{M}$ with increasing the concentration of quinoline derivatives (1) (0, 10, 20, 30, 40, and $50 \mu\text{M}$).

Fluorescence quenching measurements

The fluorescence emissions can be generated by aromatic amino acid chromophores, such as Trp and Phe, in the protein that Tryptophan has the highest fluorescence intensity among the amino acid residues. Moreover, the fluorescence sensitivity depends on the environment surrounding the chromophore in the protein. Therefore, the fluorescence of tryptophan residue can be applied as a fluorescent probe to investigate drug-protein binding interaction. The fluorescence-quenching constant (K_{sv}) of the serum albumin, which was incorporated with (1) and (2), were determined by using Stern-Volmer equation (equation 4).

$$\frac{F_0}{F} = 1 + K_{sv}[Q] = 1 + K_q \tau_0 \quad \text{---- [4]}$$

BSA and HSA have fluorescence lifetimes approximately as 6 and 5.60 ns, respectively (Dufour, Roger, & Haertle, 1992). Ksv value was taken from the plot slope between F_0 / F and $[Q]$. $[Q]$ indicates the initial quencher concentration. If the quenching constant increases with higher temperatures, the quenching mechanism can be regarded as dynamic quenching, although quenching depends mainly on molecular collisions. Static quenching can be allocated if the quenching constant decreases with higher temperature, under which the stability of the complex structure is lower at a higher temperature. In this research, the protein's fluorescence quenching mechanism was confirmed using temperature dependence (Ware, 1962). The serum albumin fluorescence emission spectra were recorded in the presence of (1) (Figure 39) or (2) (Figure 40). Serum albumin displayed a strong peak of fluorescence at 340 nm with an excitation wavelength of 285 nm. The results showed a decrease in the fluorescence intensity of serum albumin when compound (1) and compound (2) concentrations were increased, indicating that changing of the surrounding environment of Trp residues in the protein were induced upon binding to compound (1) and compound (2). The KSV values of serum albumin, which incorporating with the compound (1) and compound (2) were determined using the Volmer – Stern equation. Table 1 presents the results of the BSA and HSA Stern – Volmer quenching constants with compound (1) at three different temperatures, and Table 2 shows the results of Stern – Volmer serum albumin with compound (2) quenching constants at three different temperatures. The K_{sv} values of BSA and HSA with compound (1) decreased as the temperature increased, indicating that the quenching mechanism demonstrated with serum albumin as a static quenching mechanism of compound (1). The KSV values of serum albumin with compound 2 also exhibited the same quenching mechanism, with increasing temperature, the KSV values decreased. The biomolecule's maximum collisional quenching constant is $2.0 \times 10^{10} \text{ Lmol}^{-1}\text{s}^{-1}$, which is the value of the occurrence of a dynamic quenching mechanism. However, the K_q values of serum

albumin with compound (1) and compound (2) was substantially greater than the mean biomolecule collisional quenching constant. Therefore, the binding mechanism between compound serum albumin (1) and with compound (2) was static quenching mechanism (Abou-Zied & Al-Shihi, 2008).

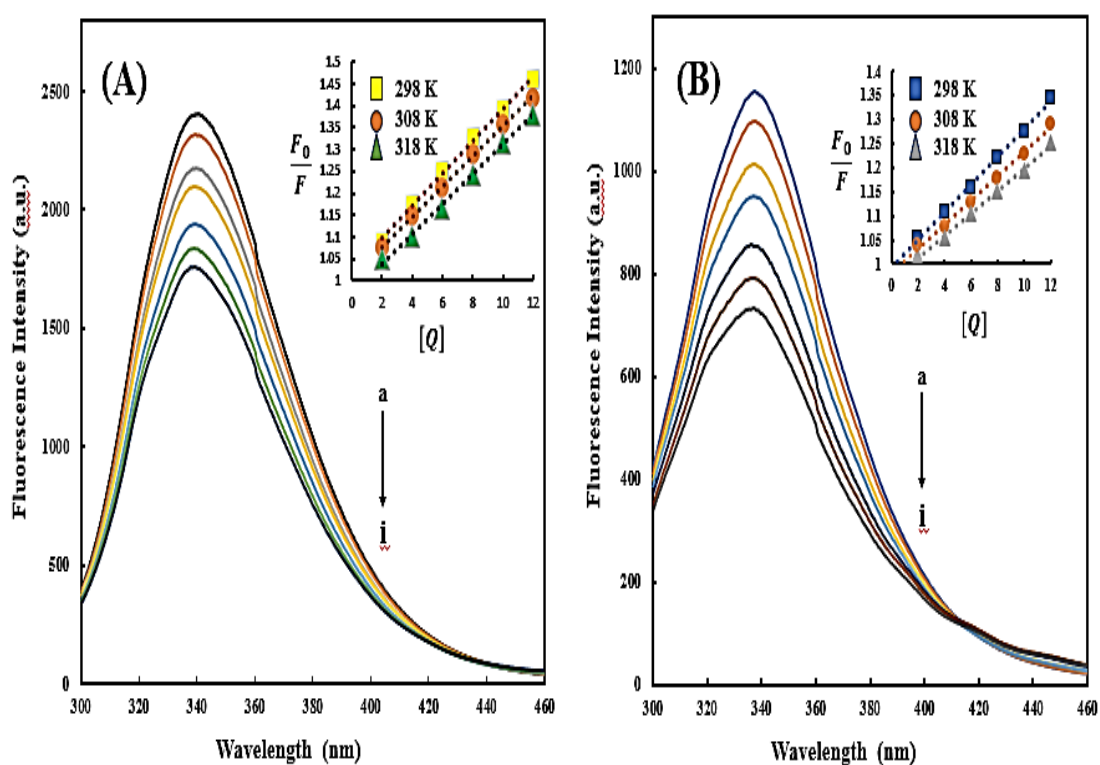


Figure 39 The emission spectra of BSA (A) and HSA (B) with the increasing concentration of (1).

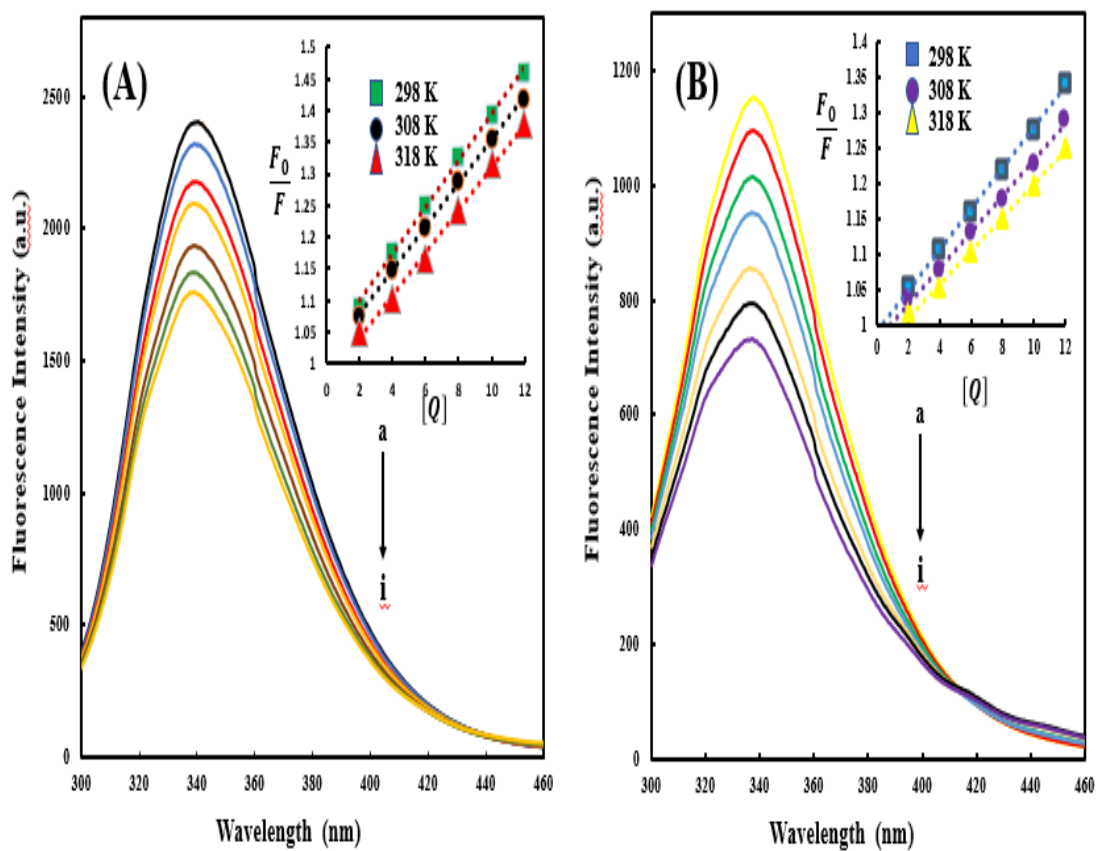


Figure 40 The spectra of BSA (A) and HSA (B) with the increasing concentration of (2).

Table 1 Stern–Volmer quenching constants of serum albumin with compound 1 at three different temperatures.

BSA			HSA		
Temperature (K)	K_{SV} (L.mol ⁻¹) x 10 ⁴	R ²	Temperature (K)	K_{SV} (L.mol ⁻¹) x 10 ⁴	R ²
298	3.68	0.9975	298	2.88	0.9982
308	3.45	0.999	308	2.52	0.9961
318	3.39	0.9967	318	2.35	0.9971

R² is the correlation coefficient for Stern–Volmer equation.

Table 2 Stern–Volmer quenching constant of BSA and HSA with compound 2 at three different temperature system.

BSA			HSA		
Temperature (K)	K_{SV} (L.mol ⁻¹) x 10 ⁴	R ²	Temperature (K)	K_{SV} (L.mol ⁻¹) x 10 ⁴	R ²
298	3.24	0.9925	298	2.68	0.9912
308	2.95	0.990	308	2.21	0.9901
318	2.51	0.9914	318	1.97	0.9950

R² is the correlation coefficient for Stern–Volmer equation.

Binding constant and number of binding site

The binding constants and the binding site number were analyzed using equation 5. The binding constants (K_b) of serum albumin with compound (1) or compound (2) were evaluated by using the plot between $\log \left(\frac{F_0 - F}{F} \right)$ and $\log[Q]$. Figure 41 shows the plot of serum albumin with compound (1) and Figure 42 shows the plot of serum albumin with compound (2). The results were calculated and listed in Tables 3 and 4. At three different temperatures, the K_b values demonstrated in the between of 104- 105 L. mol⁻¹. The results showed that the binding interaction between BSA and HSA with (1) and with (2) showed strong binding interaction. Moreover, the number of the binding site for serum albumin-ligand was 1 due to the ratio for the complexation between serum albumin and the compound displayed 1:1 ratio.

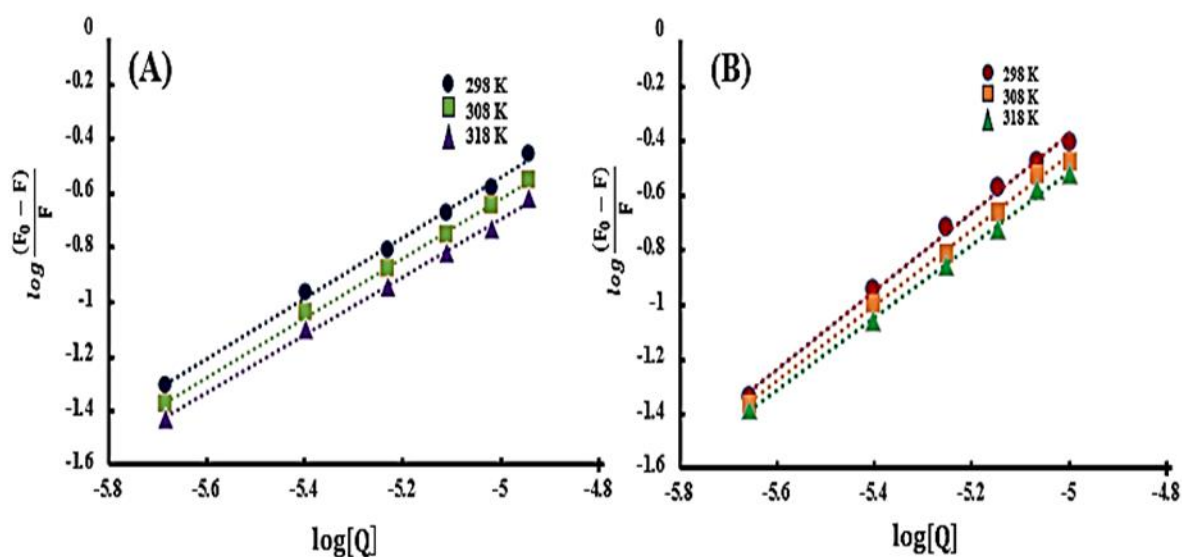


Figure 41 Plot of the quenching interaction of BSA (A) and HSA (B) with (1).

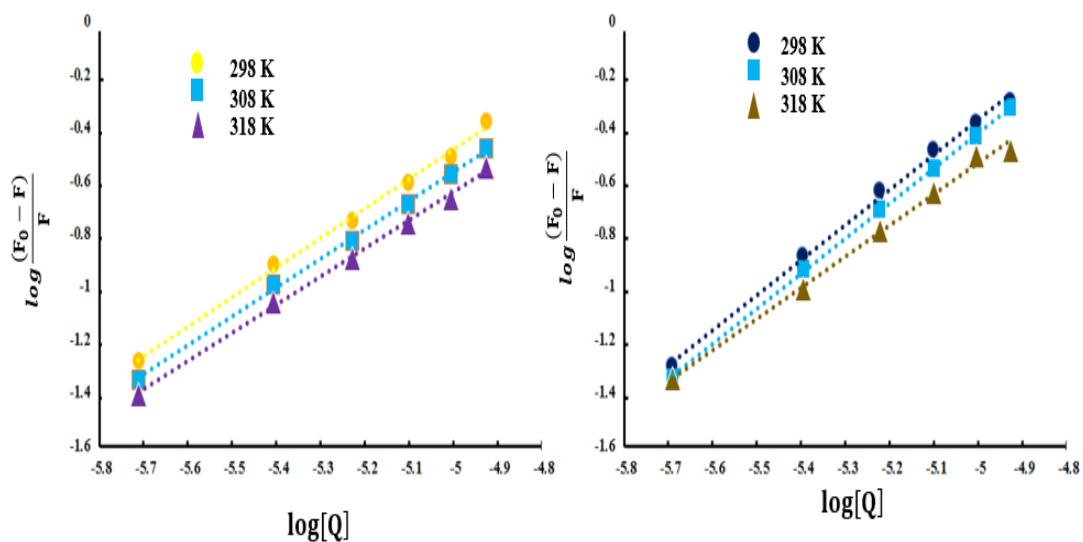


Figure 42 Plot of the quenching interaction of BSA (A) and HSA (B) with (2).

Table 3 Binding constants and the number of binding site of serum albumin with (1) at three different temperatures.

Temperature (K)	BSA			HSA		
	Kb (L.mol ⁻¹)	n	R ²	Kb (L.mol ⁻¹)	n	R ²
298	1.27 × 10 ⁵	1.13	0.996	1.07 × 10 ⁵	1.14	0.996
308	6.35 × 10 ⁴	1.08	0.997	6.87 × 10 ⁴	1.09	0.998
318	3.71 × 10 ⁴	1.05	0.998	4.10 × 10 ⁴	1.06	0.997

Table 4 Binding constants and the number of binding site of serum albumin with (2) at three different temperatures.

Temperature (K)	BSA			HSA		
	K_b (L.mol ⁻¹)	n	R ²	K_b (L.mol ⁻¹)	n	R ²
298	1.06×10^5	1.08	0.995	9.23×10^4	1.03	0.995
308	5.24×10^4	1.12	0.994	6.87×10^4	1.13	0.990
318	2.96×10^4	1.01	0.998	4.10×10^4	1.07	0.991

The thermodynamic parameter and the binding mode

From the reported binding mode between small molecule and protein, there are mostly 4 types of interactions; known as electrostatic interaction, H bonding interaction, hydrophobic interaction, and van der Waals force. The thermodynamic parameter signs, Gibbs free energy (ΔG), enthalpy change (ΔH), and entropy change (ΔS), in the ligand-protein binding process can be established to evaluate the binding mode. Typically, when both enthalpy change (ΔH) and entropy change (ΔS) values have a positive signal, the hydrophobic interaction force is indicated. If the values of enthalpy change (ΔH) and entropy change (ΔS) are both negative signals, the interaction force of van der Waals force or H-bonding interaction can be determined. Apart from that, in part of enthalpy change (ΔH) value zero and entropy change (ΔS) with a positive signal, an electrostatic force is determined for the main interaction (Ross & Subramanian, 1981b). The thermodynamic parameters in the ligand-protein binding mode can be evaluated with the Van't Hoff equations (equation 7).

$$\Delta G = -RT \ln K_b \quad \text{---- [6]}$$

$$\ln K_b = -\frac{\Delta H}{RT} + \Delta S/R \quad \text{---- [7]}$$

These thermodynamic parameters for BSA and HSA binding with (1) were obtained from the $\ln K_b$ and $1/T$ plot as shown in Figure 43, while the same BSA and HSA binding plot was obtained with (2) as shown in Fig 44. The results of the thermodynamic parameters are described in Tables 5, 6, 7, and 8. The values of enthalpy change (ΔH) and entropy change (ΔS) were shown as $-48.5 \text{ kJ mol}^{-1}$, $-65.21 \text{ J mol}^{-1}\text{K}^{-1}$, respectively and The value of Gibbs free energy (ΔG) was shown as $-29.07 \text{ kJ mol}^{-1}$ at 299 K, in the case of BSA binding with (1) (Table 5). enthalpy change (ΔH) and entropy change (ΔS) values were $-44.55 \text{ kJ mol}^{-1}$, $-51.80 \text{ J mol}^{-1} \text{ K}^{-1}$, respectively and ΔG value was demonstrated as $-29.09 \text{ kJ mol}^{-1}$ at 299 K, in part of HSA binding with (1) (Table 6). enthalpy change (ΔH) and entropy change (ΔS) values were demonstrated as $-41.12 \text{ kJ mol}^{-1}$, $-53.41 \text{ J mol}^{-1}\text{K}^{-1}$, respectively and Gibbs free energy (ΔG) value was demonstrated as $-25.97 \text{ kJ mol}^{-1}$ at 299 K, in the case of BSA binding with (2) (Table 7). enthalpy change (ΔH) and entropy change (ΔS) values were $-40.96 \text{ kJ mol}^{-1}$ and $-48.72 \text{ J mol}^{-1} \text{ K}^{-1}$, respectively and Gibbs free energy (ΔG) value was demonstrated as $-26.44 \text{ kJ mol}^{-1}$ at 299 K, in the case of HSA binding with (2) (Table 8). It was concluded that the principal force of interaction between (1) and serum albumin emerged spontaneously and exhibited van der Waals force or H bonding interaction. In addition, the main interaction between (2) and serum albumin showed the same van der Waals force or H bonding interaction.

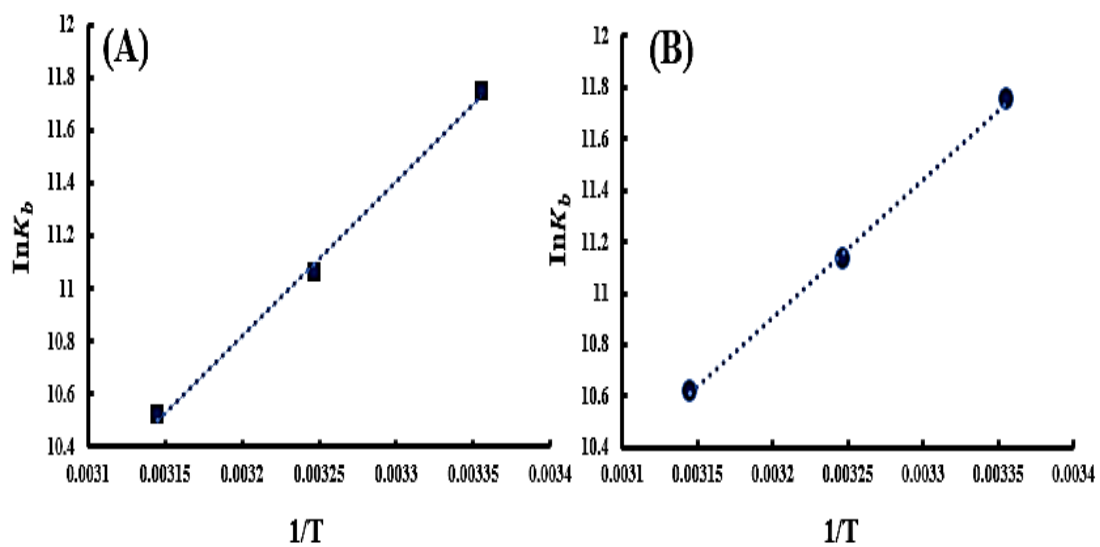


Figure 43 Van't Hoff plot for the binding interaction of BSA with (1) (A), and HSA with (1) (B).

Table 5 The parameters of thermodynamic of the binding between BSA and (1).

Temperature (K)	ΔH (kJ mol ⁻¹)	ΔS (J mol ⁻¹ K ⁻¹)	ΔG (kJ mol ⁻¹)	R ²
298	-48.5	-65.21	-29.07	0.9973
308			-28.42	
318			-27.76	

Table 6 The parameters of thermodynamic of the binding between HSA and (1).

Temperature (K)	ΔH (kJ mol ⁻¹)	ΔS (J mol ⁻¹ K ⁻¹)	ΔG (kJ mol ⁻¹)	R ²
298	-44.55	-51.89	-29.09	0.9986
308			-28.57	
318			-28.05	

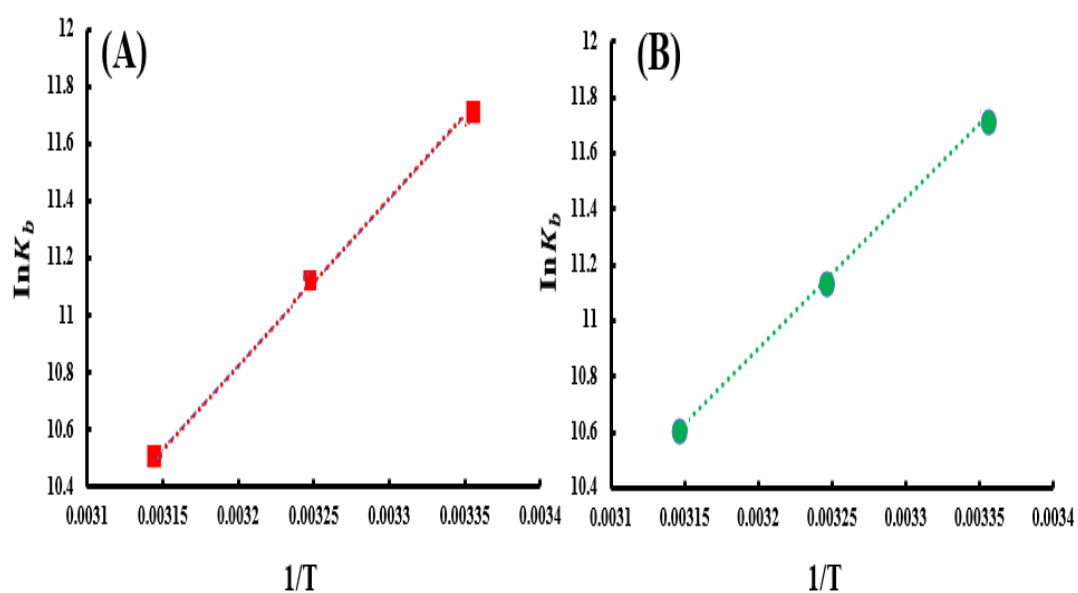


Figure 44 Van't Hoff plot for the binding of BSA with (2) (A), and BSA with (2) HSA (B).

Table 7 The thermodynamic parameter of the binding between BSA and (2).

Temperature (K)	ΔH (kJ mol ⁻¹)	ΔS (J mol ⁻¹ K ⁻¹)	ΔG (kJ mol ⁻¹)	R
298	-41.12	-53.41	-25.97	0.9954
308			-26.42	
318			-26..12	

Table 8 The thermodynamic parameters of the binding between HSA and (2).

Temperature (K)	ΔH (kJ mol ⁻¹)	ΔS (J mol ⁻¹ K ⁻¹)	ΔG (kJ mol ⁻¹)	R ²
298	-40.96	-48.72	-26.44	0.9914
308			-25.91	
318			-26.35	

Competitive binding between (1), warfarin and ibuprofen to serum albumin.

In the literature previously published, binding ligand sites on BSA and HSA were located in the hydrophobic pocket of subdomains IIA or site I, and subdomains IIIA or site II, respectively. The ligand-binding site of interesting ligand on the protein can be determined by performing the site marker competition. Site marker: Warfarin and ibuprofen are the known specific ligands bound with the known binding sites on serum albumin. Warfarin was demonstrated as binding site marker for sub-domain IIA, whereas ibuprofen was found to be a binding site marker for sub-domain IIIA. The competitive binding was performed by using fluorescence measurements (Wu et al., 2011). In the absence and presence of the site marker, the binding constants (K_b) of (1) and (2) with serum albumin were determined according to equation (2) and listed in Tables 9 and 10. The results confirmed that the K_b values of BSA with compound (1) and with compound (2) and the K_b values of HSA with compound (1) and with compound (2), in the part of warfarin as a site marker at room temperature, in the absence of the site marker (blank)

were lower than that of serum albumin with (1) or (2), while at room temperature the K_b value of BSA or HSA with the quinoline derivatives in ibuprofen component indicated no difference from the blank. Therefore, there was a competition binding between the quinoline derivatives and warfarin, concluding that the binding site of com (1) and com (2) with serum albumin was mainly binding site within sub-domain IIA.

Table 9 Binding constants of serum albumin with (1) in the presence of the site markers.

Ligand	BSA		HSA	
	$\log K_b$	R^2	$\log K_b$	R^2
(1)	5.1051	0.996	5.0293	0.9968
warfarin	4.3752	0.9967	4.3315	0.9911
ibuprofen	5.1449	0.9971	5.0054	0.9973

Table 10 Binding constants of serum albumin with (1) in the presence of the site markers.

Ligand	BSA		HSA	
	$\log K_b$	R^2	$\log K_b$	R^2
(2)	5.1026	0.9913	5.0146	0.9954
warfarin	4.2932	0.9945	4.3427	0.99
ibuprofen	5.1031	0.9921	5.013	0.9968

Molecular docking of compounds 1 and 2 with serum albumin

Molecular docking is a predictive technique for the binding site, binding energy, and binding interaction with serum albumin between (1) and (2) to support spectroscopic experiment results. In this study, molecular docking has been used to determine the binding mechanism of quinoline derivatives at the BSA and HSA binding sites to obtain a

better understanding of the proper functioning of quinoline derivatives as candidate drugs. BSA and HSA have the most similar amino acid sequence and a similar structure. The binding energies of compound (1) and compound (2), upon binding to serum albumin, were determined as shown in Table 11.

Table 11 Binding energy (BE) of serum albumin with (1) and (2) by using molecular docking.

Ligand	BSA		HSA	
	Binding energy of site I (kcal mol)	Binding energy of site II (kcal mol)	Binding energy of site I (kcal mol)	Binding energy of site II (kcal mol)
Compound (1)	-10.34	-8.7	-10.14	-7.47
Compound (2)	-9.42	-8.13	-9.26	-8.26
Warfarin	-9.28	-7.76	-8.80	-8.07
Ibuprofen	-7.54	9.12	-6.54	-8.64

The results implied that the binding energy of the quinoline derivatives binding to serum albumin on site I was more negative than these compounds binding to BSA and HSA on-site II. The binding energies of BSA and HSA with quinoline derivatives were more negative than that of serum albumin with warfarin. Thus, compound (1) and compound (2) bonded to serum albumin subdomain IIA, in which the binding of these compounds to BSA and HSA indicated stronger interaction than that of warfarin to BSA and HSA, corresponding to the competitive binding experiments.

The results of molecular docking are shown in Figures 45-48 (1) and (2) serum albumin binding to a hydrophobic pocket in subdomain IIA (Figures 45A, 46A, 47A, and 48A). The amino acids surrounding (1) within the radius of 3.0 Å of serum albumin. Two H bonds were formed between BSA and compound (1) which were found between the H atom of the NH₂ group in Arg347 (2.901 Å) and the N atom of CN group in compound (1)

and between the NH₂ group atom H in Lys350 (1.843 Å) and the N atom of CN in compound (1). Trp213 residue showed π - π stacking interaction (2.477 Å) with benzene ring of compound (1) (Figure 45B). In the case of HSA binding with compound (1), three H bonds were formed between the O atom of C=O group on Ala210 and the H atom of the amine group in compound (1) (2.171 Å), between the H atom of Ser202 hydroxyl group and the N atom of cyanide in compound (1) (2.720 Å), and between the H atom of Lys350 hydroxyl group and N atom of cyanide in compound (1) (2.171 Å). In addition, Trp214 showed π - π stacking interaction (2.343 Å) with the benzene ring of compound (1) (Figure 46B).

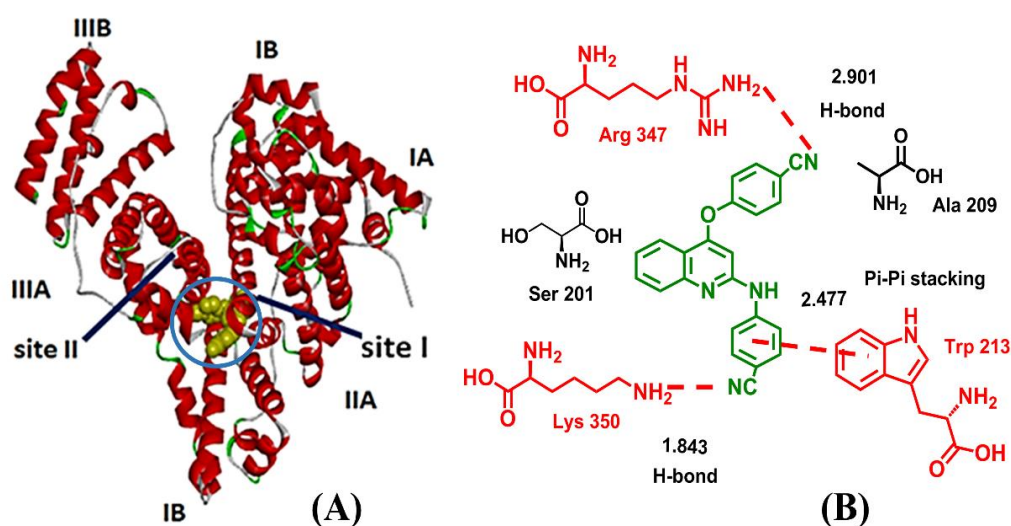


Figure 45 (A) The conformation of (1) of BSA. (B) The amino acids of BSA.

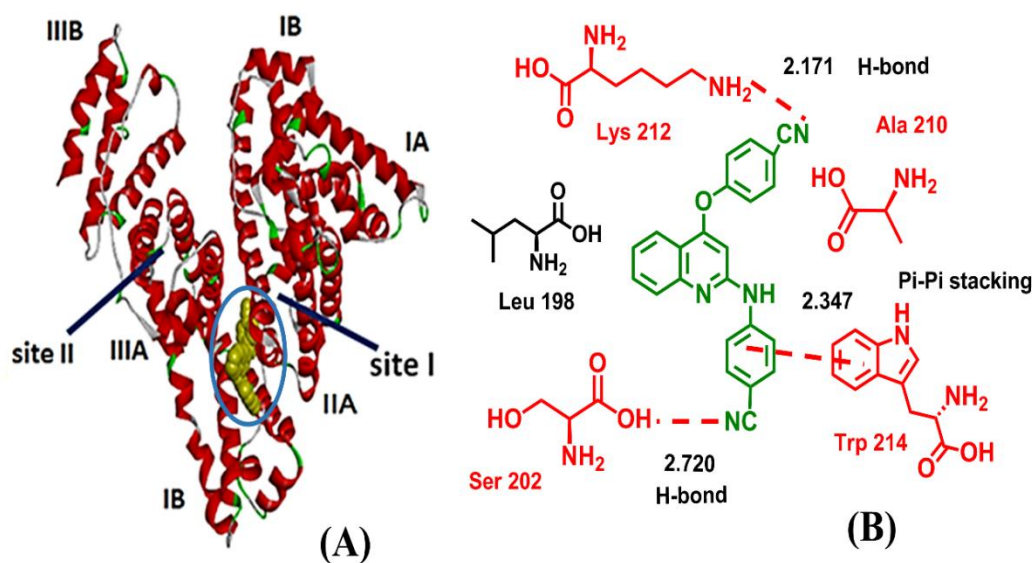


Figure 46 (A) The conformation of (1) of HSA. (B) The amino acids of HSA.

The results of docking between compound (2) with BSA indicated 5 amino acids, Ala209, Trp213, Arg483, Arg484 and Lys350, surrounding compound (2) within the radius of 3.0 Å, while compound (2) was surrounded by Tyr150, Ser193, Gln196, Trp214 and His242 in HSA) within 3.0 Å. Two H bonds were formed for BSA and compound 2 which was found between the H atom of the amine group in Arg343 and the N atom of CN group in compound (2) (2.193 Å) and between the NH₂ group atom H in Arg384 and the N atom of CN group in compound (2) (2.082 Å). Trp213 residue demonstrated pi-pi stacking interaction (3.814 Å) with benzene ring of compound (2) (Figure 47B). In the part of HSA with the compound (2), two H bonds were formed between the H atom of the amine group in His242 and the nitrogen atom of cyanide in compound (2) (2.237 Å), and between the H atom of the hydroxyl group in Ser193 and the N atom of CN group in compound (2) (2.657 Å). Trp214 demonstrated π - π stacking interaction (3.662 Å) with the benzene ring of compound (2) (Figure 48B).

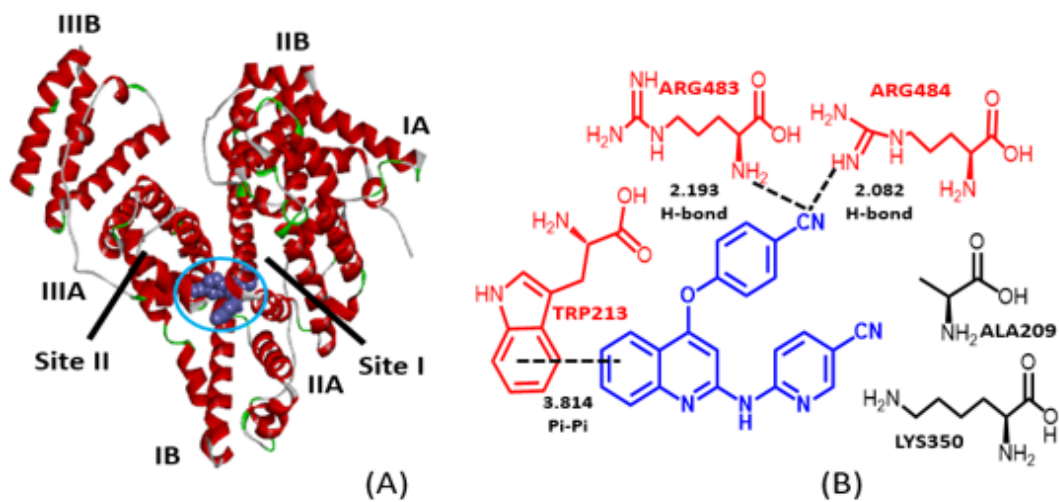


Figure 47. (A) The conformation of 4 (2) of BSA. (B) The amino acids of BSA.

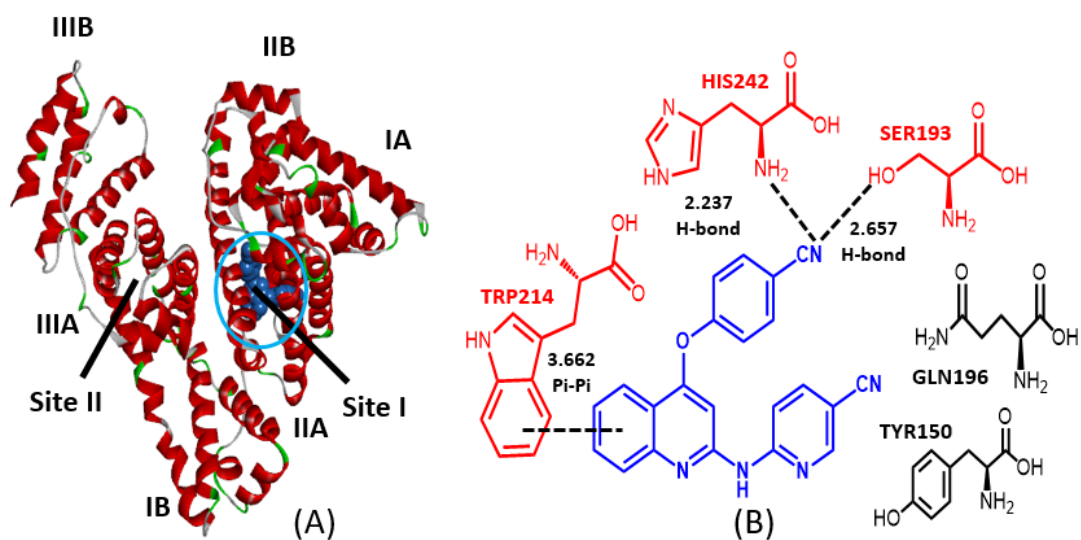


Figure 48. (A) The conformation of (2) of BSA. (B) The amino acid of HSA.

The effect of π - π interactions conformed to the results of UV-VIS spectroscopy, which showed that absorption increased when compound concentrations were increased (1) and (2). Therefore, the binding site of serum albumin with compound (1) and with compound (2) could be bind to subdomain IIA, and the main interactions were H bonding forces and van der Waals. From the study, compound (1) binding to serum albumin gave better binding energy values than that of compound (2), and the amino acids surrounding the ligand were different. Therefore, compound (1) can be considered to bind to serum albumin better than compound (2), consistent with the previous report, in which the percentage inhibitory activity of HIV-1 by compound (1) was found to be higher than that of compound (2). (Makarasen et al., 2019, pp. 671-682).

Molecular docking of 2,4-disubstituted quinoline derivatives with serum albumin

From the previously reported literature, amino-oxy-diarylquinoline derivatives were synthesized and evaluated from a combination of the pharmacophore templates of etravirine (ETV, TMC125), nevirapine, efavirenz, and rilpivirine (Makarasen et al., 2019, pp. 671-682). These compounds were divided into two groups: 4,6-disubstituted quinoline derivatives and 2,4-disubstituted quinoline derivatives, and the synthesized compounds have been evaluated for HIV-1 RT inhibitors. The study showed the potential of 2,4-disubstituted quinoline derivatives to interact and bind to HIV-1 RT because they were consistent in the same arrangement, making it more suitable for studying and designing target molecules than 4,6-disubstituted quinoline derivatives. The Inhibition (%) against HIV-1 RT are shown in Table12. In this research, the binding interaction between 2,4-disubstituted quinoline derivatives with serum albumin by molecular docking were investigated (Figure 49). The interaction of 2,4-disubstituted quinoline derivatives with serum albumin can be further used as a guideline for the future evolution of HIV-1 RT inhibitors.

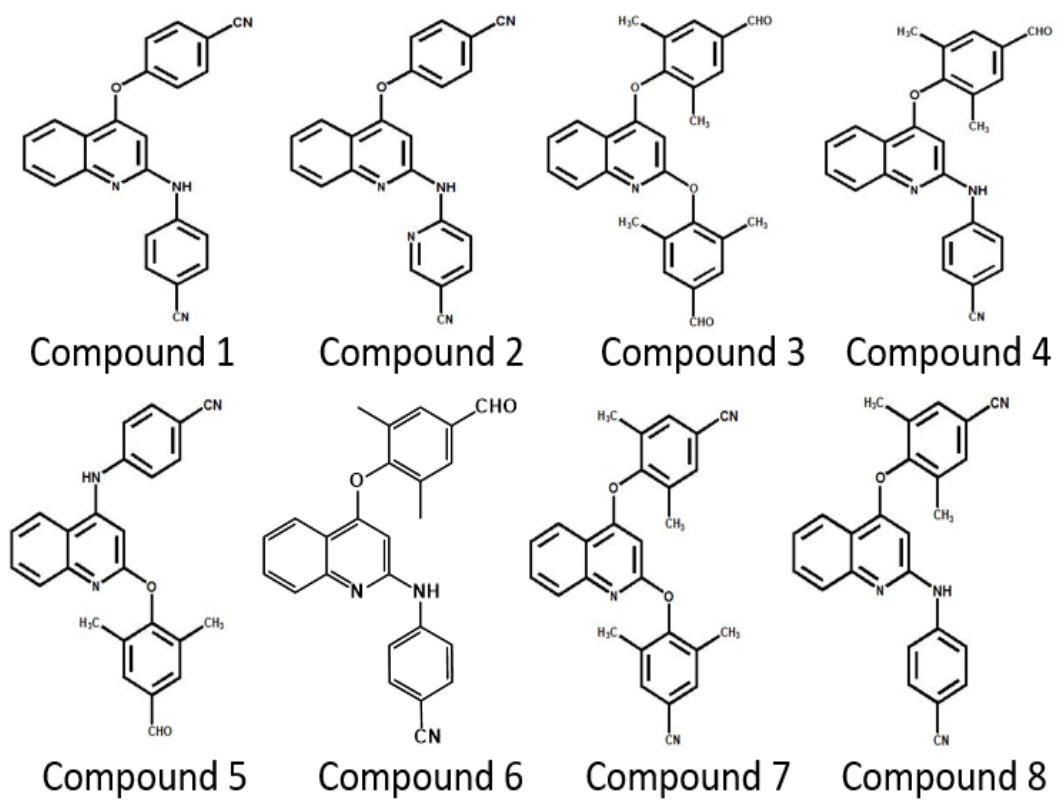


Figure 49 The structures of quinoline derivatives.

Table 12 Inhibitory activity (%) of the 2,4-disubstituted quinoline derivatives (1 μ M) against HIV-1 RT

2,4-disubstituted quinoline derivatives	Inhibition (%) against HIV-1 RT
Compound 1	39.71
Compound 2	27.60
Compound 3	42.08
Compound 4	43.37
Compound 5	-
Compound 6	62.23
Compound 7	40.31
Compound 8	47.16

The molecular docking results are shown in Figures 49-60. The quinoline derivatives bind to the serum albumin hydrophobic pocket in subdomain IIA (Figures 49A, 50A, 51A, 52A, 53A, 54A, 55A, 56A, 57A, 58A, 59A, and 60A). The molecular docking results concluded that the binding energy of the quinoline derivatives binding to a site I (subdomain IIA) was more negative than the quinoline derivatives binding to site II (subdomain IIIA). Table 12 shows the binding energies between serum albumin with 2,4-disubstituted quinoline derivatives. The binding energy of serum albumin with 2,4-disubstituted quinoline derivatives was more negative than that of serum albumin with warfarin. Thus, the 2,4-disubstituted quinoline derivatives have a higher potential to bound to subdomain IIA of BSA and has than warfarin.

Table 13 Binding energy of serum albumin with 2,4-disubstituted quinoline derivatives by using molecular docking

2,4- disubstituted quinoline derivatives	BSA		HSA	
	Binding energy of site I (kcal/mol)	Binding energy of site II (kcal/mol)	Binding energy of site I (kcal/mol)	Binding energy of site II kcal/mol)
(3)	-10.68	-8.93	-10.31	-7.62
(4)	-10.70	-8.85	-9.97	-8.21
(5)	-10.31	-8.74	-10.01	-8.14
(6)	-11.07	-9.13	-10.82	-8.82
(7)	-10.75	-9.11	-10.19	-8.32
(8)	-10.83	-9.06	-10.28	-8.71
Warfarin	-9.48	-7.76	-8.80	-8.07
Ibuprofen	-7.54	9.12	-6.54	-8.64

The docking results indicated that compound (3) was surrounded by the amino acids; Arg208, Trp213, Leu346, Arg347 and Pro485 upon binding to BSA, and surrounded by the amino acids; Tyr150, Lys195, Gln196, Trp214 and Ser287 upon binding to HSA, within 3.0 Å. Three H bonds were formed between compound (3) and BSA, in which the H atom of the amine group in Arg347 bonded to the O atom of C=O group in compound (3) (1.956 Å), the H atom of a hydroxyl group in Pro485 bonded to the O atom of C=O group in compound (3) (2.904 Å), and the H atom of the amine group in Arg208 bonded to the O atom of C=O group in compound (3) (2.158 Å). Trp213 demonstrated π - π stacking interaction (2.752 Å) with benzene ring of compound (3) (Figure 50B). In case of HSA, two H bonds were also observed between H atom of the hydroxyl group in Ser287 and the O atom of C=O group in compound (3) (2.959 Å) and between H atom of the amine group on Lys195 and the O atom of C=O group in

compound (3) (2.349 Å). Trp214 also demonstrated π - π stacking interaction (2.854 Å) with the benzene ring of compound (3) (Figure 51B).

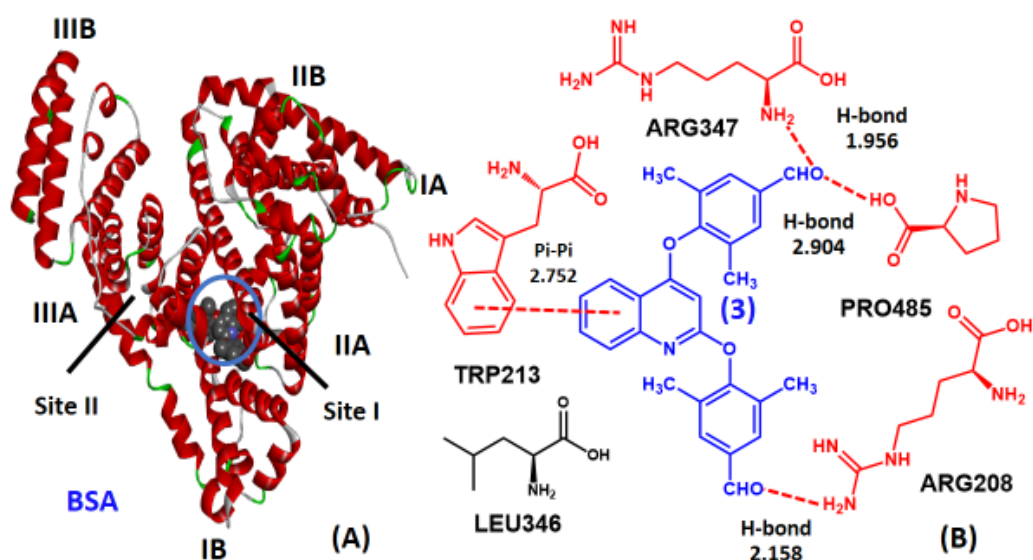


Figure 50 (A) The conformation of compound 3 of BSA. (B) The amino acids on BSA.

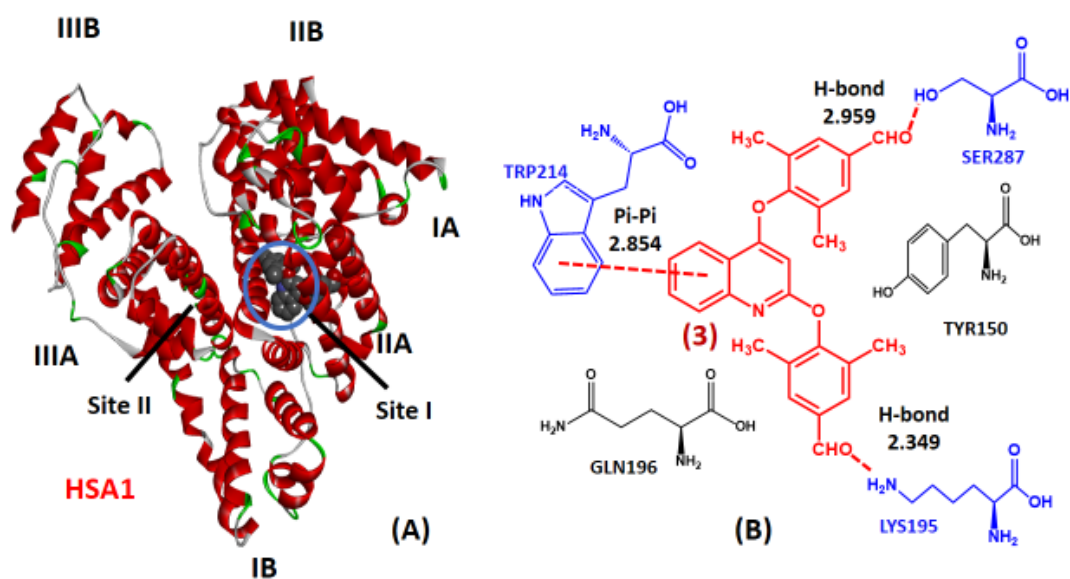


Figure 51 (A) The conformation of compound 3 of HSA. (B) The amino acids on HSA.

The docking results between compound (4) with serum albumin indicated that compound (4) was surrounded by amino acids; Trp213, Leu346, Arg347, LYS350 and Pro485 within 3.0 Å, upon binding to BSA, and surrounded by amino acids; Tyr150, Ser193, LYS195, Gln196, and Trp214, upon binding to HSA. Two H bonds were formed for BSA and compound (4), in which the H atom of the amine group in Arg347 bonded to the O atom of C=O group in compound (4) (1.834 Å), and the H atom of the hydroxyl group in Pro485 bonded to the O atom of C=O group in compound (4) (3.080 Å). Trp213 residue demonstrated π - π stacking interaction (3.014 Å) with benzene ring of compound (4) (Figure 52B). In case of HSA, two H bonds were also involved in the binding interactions, in which the H atom of the hydroxyl group in Tyr150 bonded to the N atom of CN group in compound (4) (2.158 Å), and the H atom of Hydroxyl group on Ser193 bonded to the O atom of C=O group in compound (4) (2.842 Å). Trp214 also demonstrated π - π stacking interaction (2.621 Å) with the benzene ring of compound (4) (Figure 53B).

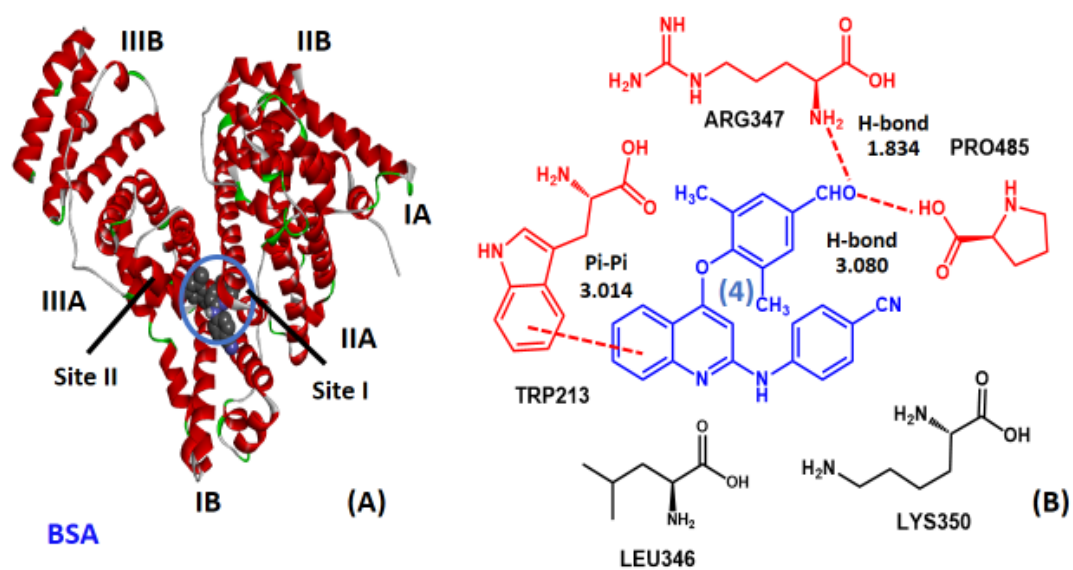


Figure 52 (A) The conformation of compound 4 of BSA. (B) The amino acids on BSA.

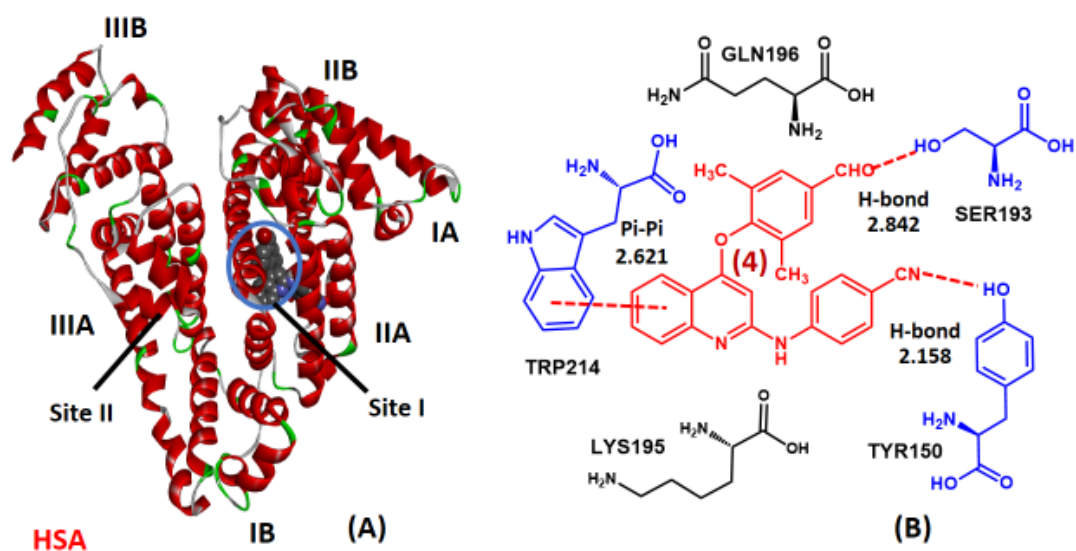


Figure 53 (A) The conformation of compound 4 of HSA. (B) The amino acids on HSA.

The docking results between compound (5) with serum albumin indicated that compound (5) was surrounded by amino acids; as Arg194, Ser201 Trp213 and Arg483 within 3.0 Å, upon binding to BSA, and surrounded by amino acids; Tyr150, Lys193, Gln196, Trp214, and Ala291, upon binding to HSA. Two H bonds were formed for BSA and compound (5) in which the H atom of the amine group in Arg194 bonded to the N atom of CN group in compound (5) (2.325 Å), and the H atom of the amine group in Arg483 bonded to the O atom of C=O group in compound (5) (2.341 Å). Trp213 residue demonstrated π - π stacking interaction (3.173 Å) with benzene ring of compound (5) (Figure 54B). In case of HSA, two H bonds were also involved in the binding interactions, in which the H atom of the hydroxyl group in Tyr150 bonded to the O atom of C=O group in compound (5) (2.943 Å), and the H atom of NH₂ group in Ala291 bonded to the N atom of CN group in compound (5) (2.957 Å). Trp214 also demonstrated π - π stacking interaction (3.173 Å) with the benzene ring of compound (5) (Figure 55B).

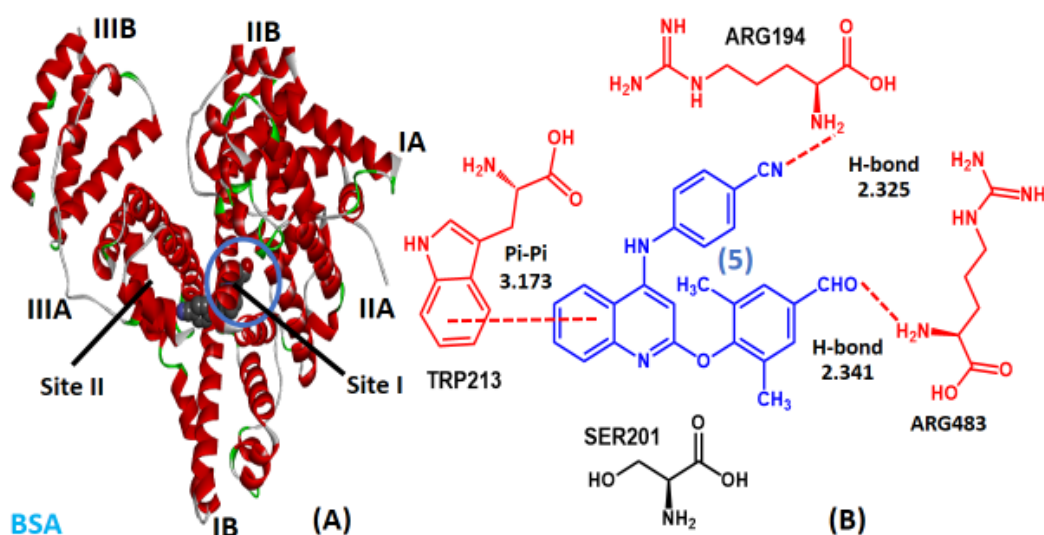


Figure 54 (A) The conformation of compound 5 of BSA. (B) The amino acids on BSA.

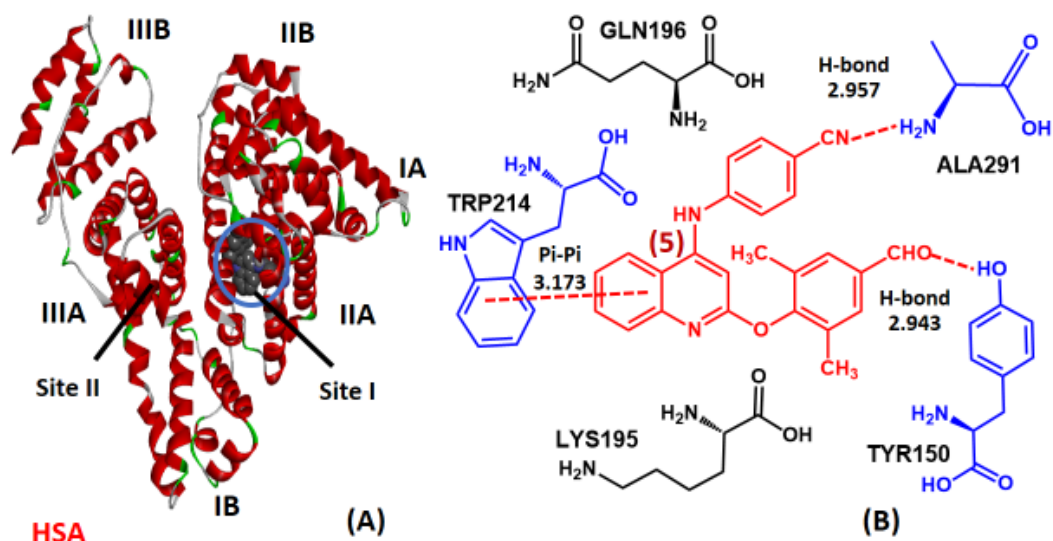


Figure 55 (A) The conformation of compound 5 of HSA. (B) The amino acids on HSA.

The docking results between compound (6) with serum albumin indicated that compound (6) was surrounded by amino acids; Trp213, Leu346, Arg347, Arg483 and Pro485 within 3.0 Å, upon binding to BSA, and surrounded by amino acids; Tyr150, Lys195, Gln196, Trp214 His242, and Arg257, upon binding to HSA. Three H bonds were formed for BSA and compound (6) in which the H atom of the hydroxyl group in Arg347 bonded to the O atom of C=O group in compound (6) (1.896 Å), the H atom of the hydroxyl group in Pro485 bonded to the O atom of C=O group in compound (6) (2.042 Å), and the H atom of a hydroxyl group in Arg483 bonded to the N atom of CN group in compound (6) (2.357 Å). Trp213 residue demonstrated π - π stacking interaction (2.957 Å) with benzene ring of compound (6) (Figure 56B). In case of HSA, three H bonds were also involved in the binding interactions, in which the H atom of the hydroxyl group in Tyr150 bonded to the O atom of C=O group in compound (6) (1.993 Å), the H atom of the amine group in Arg257 bonded to the N atom of CN group in compound (6) (2.922 Å), and the O atom of C=O group in lys195 bonded to the N atom of the amine group in compound (6) (2.996 Å). Trp214 also demonstrated π - π stacking interaction (2.965 Å) with the benzene ring of compound (6) (Figure 57B).

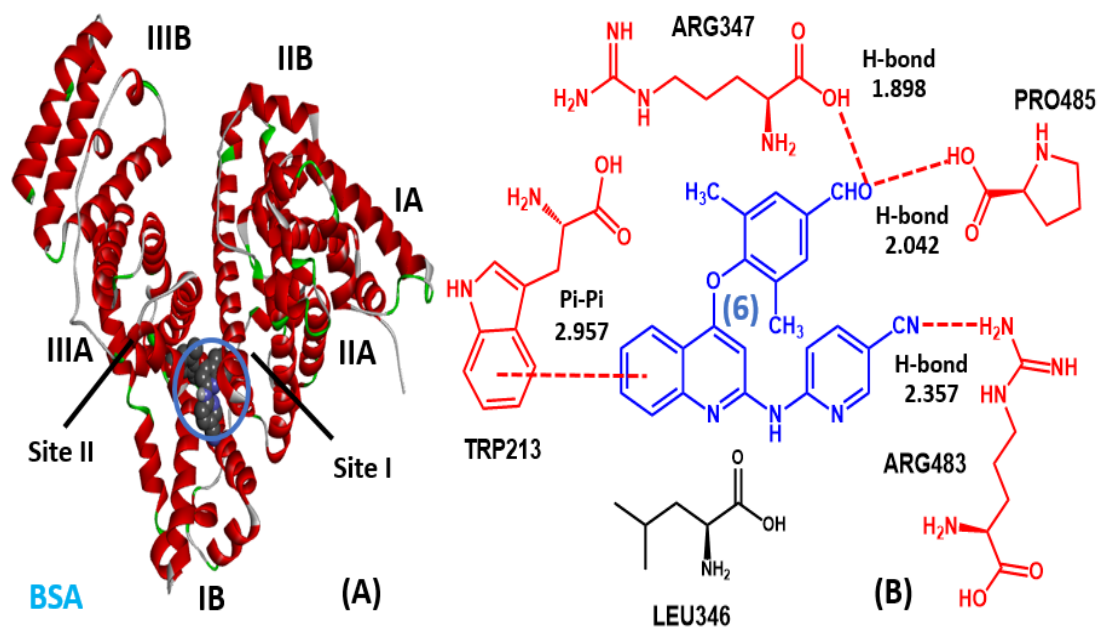


Figure 56 (A) The conformation of compound 6 of BSA. (B) The amino acids on BSA.

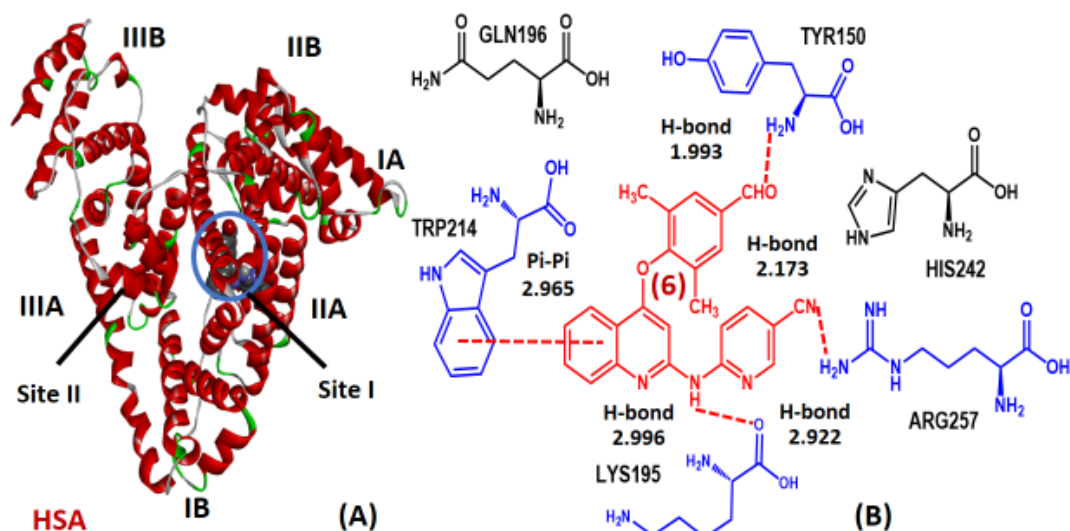


Figure 57 (A) The conformation of compound 8 of HSA. (B) The amino acids on HSA.

The docking results between compound (7) with serum albumin indicated that compound (7) was surrounded by amino acids; Ala208, Trp213, Arg483, Arg484 and Lys350 within 3.0 Å, upon binding to BSA, and surrounded by amino acids; Tyr150, Lys195, Trp214, Ser287, and Ala291, upon binding to HSA. Two H bonds were formed for BSA and compound (7) in which the H atom of the amine group in Arg208 bonded to the N atom of CN group in compound (7) (2.193 Å), and the H atom of the amine group in Arg483 bonded to the N atom of CN group in compound (7) (2.788 Å). Trp213 residue demonstrated π - π stacking interaction (3.098 Å) with benzene ring of compound (7) (Figure 58B). In case of HSA, two H bonds were also involved in the binding interactions, in which the H atom of the hydroxyl group in Tyr150 bonded to the N atom of CN group in compound (7) (2.912 Å), and the H atom of the amine group in Ala291 bonded to the N atom of CN group in compound (7) (2.831 Å). Trp214 also demonstrated π - π stacking interaction (3.662 Å) with the benzene ring of compound (7) (Figure 59B).

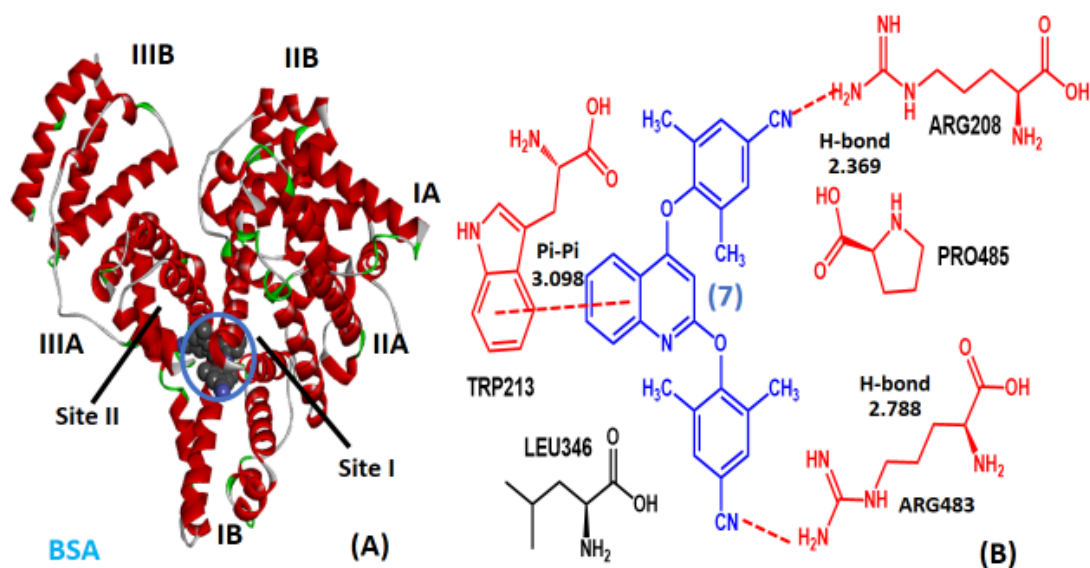


Figure 58 (A) The conformation of compound 7 of BSA. (B) The amino acids on BSA.

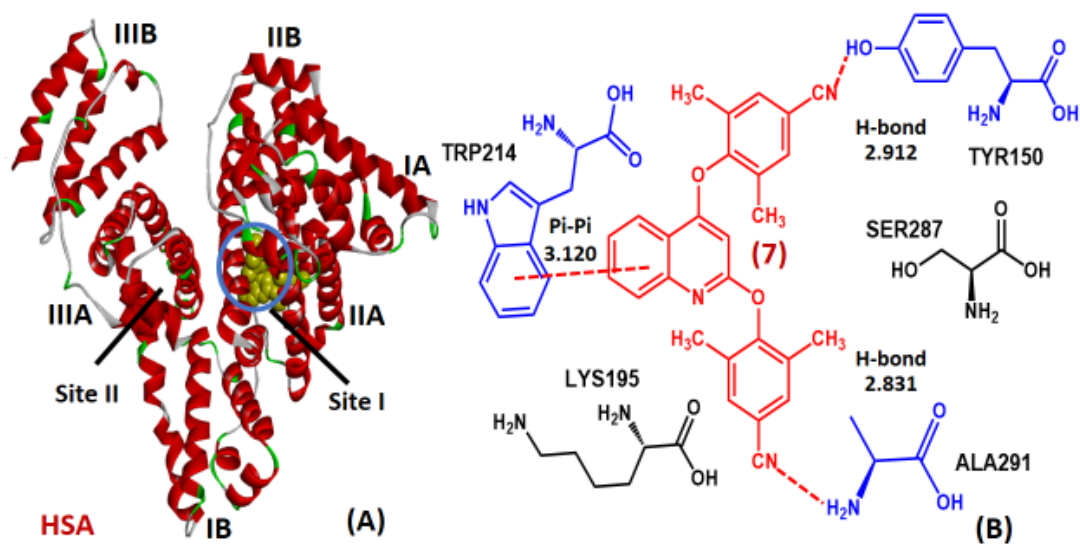


Figure 59 (A) The conformation of compound 7 of HSA. (B) The amino acids on HSA.

The docking results between compound (8) with serum albumin indicated that compound (8) was surrounded by amino acids; Trp213, Leu346, Arg347, Leu480 and Arg484 within 3.0 Å, upon binding to BSA, and surrounded by amino acids; Tyr150, Gln196, Lys199, Trp214, and Ala291, upon binding to HSA. Two H bonds were formed for BSA and compound (8) in which the H atom of the amine group in Arg347 bonded to the N atom of CN group in compound (8) (2.025 Å), and the H atom of the NH₂ group in Arg484 bonded to the N atom of CN group in compound (8) (2.145 Å). Trp213 residue demonstrated π - π stacking interaction (2.895 Å) with benzene ring of compound (8) (Figure 60B). In case of HSA, two H bonds were also involved in the binding interactions, in which the H atom of the hydroxyl group in Tyr150 bonded to the N atom of CN group in compound (8) (2.009 Å), and the H atom of NH₂ group in Ala291 bonded to the N atom of CN group in compound (8) (2.031 Å). Trp214 also demonstrated π - π stacking interaction (2.925 Å) with the benzene ring of compound (8) (Figure 61B).

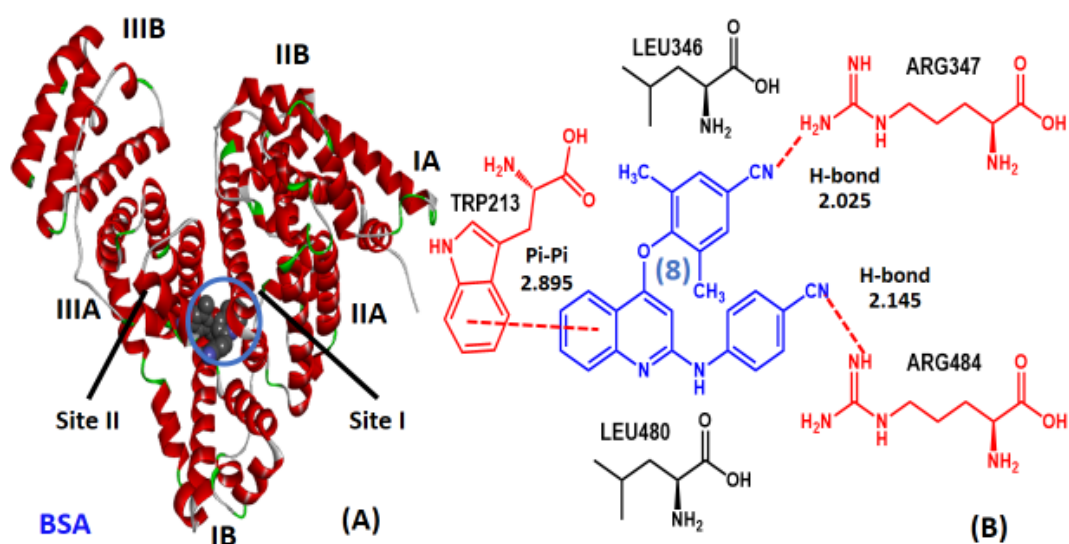


Figure 60 (A) The conformation of compound 3 of BSA. (B) The amino acids on BSA.

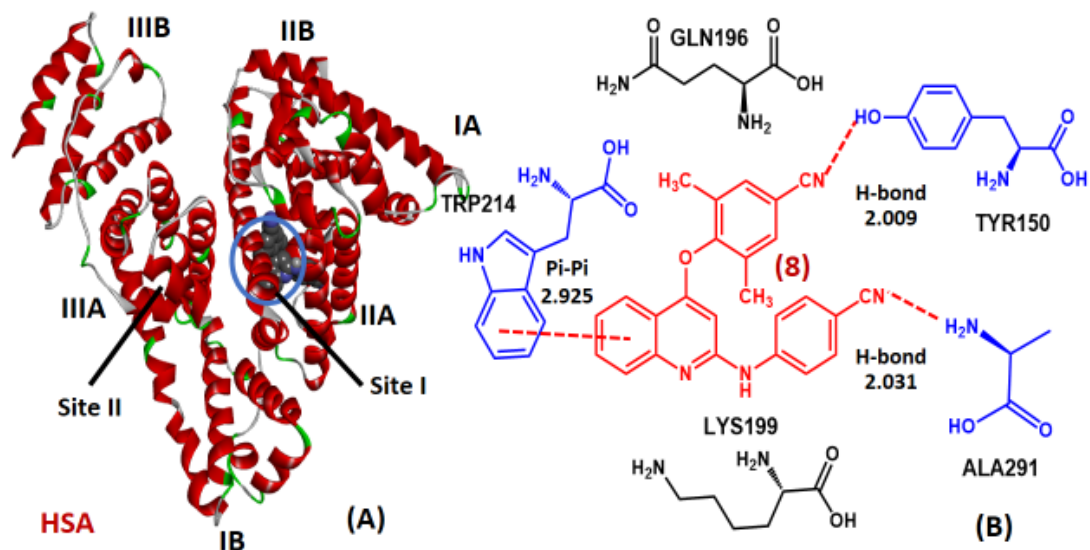


Figure 61 (A) The conformation of compound 8 of HSA. (B) The amino acids on HSA.

CHAPTER V

Conclusion

In this research, the interaction between serum albumin with (1) and (2) have been analyzed using UV – Vis spectrophotometry, fluorescence spectroscopy, competitive binding experiments, and molecular docking studies. The experimental results of the quenching procedure showed that serum albumin fluorescence has been quenched by the compound (1) and by compound (2) through a static quenching mechanism. Compound (1) bound to serum albumin with the binding constants (K_b) of 1.27×10^5 and 1.07×10^5 , respectively at 298 K, while compound (2) bound to serum albumin with the binding constants (K_b) of 1.06×10^5 and 9.23×10^4 , respectively at 298 K. The number of serum albumin binding site (n) for both compounds was 1. The binding mechanism of quinoline derivatives with serum albumin is spontaneous and the forces of interaction of both compounds with serum albumin are van der Waals force and H bonding interactions. The results of docking showed that both compounds were bind to subdomain IIA of both proteins, confirmed by the results of experiments. Docking study suggested that the compound (1) and compound (2) bound in a hydrophobic pocket with both hydrophobic and H bonding interactions through the core structure's benzene rings, the carbonyl group, and CN groups in the side chain of compounds. The effect of π π π interactions conformed to the results of UV- VIS spectroscopy, which showed that absorption increased when compound concentrations were increased (1) and (2). Therefore, the binding site of serum albumin with compound (1) and with compound (2) could be bind to subdomain IIA, and the main interactions were H bonding forces and van der Waals. From the study, compound (1) binding to serum albumin gave better binding energy values than that of compound (2), and the amino acids surrounding the ligand were different. Therefore, compound (1) can be considered to bind to serum albumin better than compound (2), consistent with the previous report, in which the percentage inhibitory activity of HIV-1 by compound (1) was found to be higher than that of compound (2). (Makarasen et al., 2019, pp. 671-682).

In the future study, the development of the structure of 2-amino-4-oxydiarylquinoline derivatives to obtain an appropriate structure and effective against HIV-1 RT inhibitors can be achieved to gain better insight into the quinoline derivatives and serum albumin interaction. Adding of an NH₂ group and a CH₃ group to the quinoline structure can be made to improve the activity of the compound. Compound (6) and Compound (8) have been selected for further studies for the binding interaction with serum albumin, as compound (6) and compound (8) have a good percentage of inhibition of HIV-1, 62.23% and 47.16%, respectively, which has the same level as NVP. The result from the molecular docking of compound (6) and compound (8) concluded that the binding site of compound (6) and compound (8) was in the cavity of a site I marker (subdomain IIA). Moreover, the docking study suggested that both hydrophobic and H bonding interactions of the aromatic rings of compound (6) and compound (8) were the main binding processes. Therefore, compound (6) and compound (8) are interesting and suitable for future studies with serum albumin. (Patnin et al., 2020).

This study can be useful for further investigation of the contribution of 2,4-disubstituted quinoline derivatives transportation. Therefore, it is expected that this research will provide valuable information for further investigations into the potential transport of new anti-HIV-1RT drugs to the target molecule.

REFERENCES

- Abadi, A. H., Hegazy, G. H., & El-Zaher, A. A. (2005). Synthesis of novel 4-substituted-7-trifluoromethylquinoline derivatives with nitric oxide releasing properties and their evaluation as analgesic and anti-inflammatory agents. *Bioorg Med Chem*, 13(20), 5759-5765.
- Abou-Zied, O. K., & Al-Shihi, O. I. K. (2008). Characterization of subdomain IIA binding Site of Human Serum Albumin in its native, unfolded, and refolded states using small molecular probes. *Journal of the American Chemical Society*, 130(32), 10793-10801.
- Asahchop, L. E., Wainberg, A. M., Sloan, D. R., & Tremblay, L. C. (2012). Antiviral drug resistance and the need for development of new HIV-1 reverse transcriptase inhibitors. . *Antimicrob Agents Chemother*, 56, 5000–5008.
- Baba, A., Kawamura, N., Makino, H., Ohta, Y., Taketomi, S., & Sohda, T. (1996). Studies on Disease-Modifying Antirheumatic Drugs: Synthesis of Novel Quinoline and Quinazoline Derivatives and Their Anti-inflammatory Effect. *Journal of Medicinal Chemistry*, 39, 5176-5182.
- C.Carter, D., & X.Ho, J. (1994). Structure of Serum Albumin. *Advances in Protein Chemistry*, 45, 153-176.
- Chander, S., Tang, C. R., Al-Maqtari, H. M., Jamalis, J., Penta, A., Hadda, T. B., . . . Sankaranarayanan, M. (2017). Synthesis and study of anti-HIV-1 RT activity of 5-benzoyl-4-methyl-1,3,4,5-tetrahydro-2H-1,5-benzodiazepin-2-one derivatives. *Bioorg Chem.*, 72, 74-79.
- Da Silva Fde, C., De Souza, M. C., Frugulhetti, I. I., Castro, H. C., Souza, S. L., de Souza, T. M., . . . Ferreira, V. F. (2009). Synthesis, HIV-RT inhibitory activity and SAR of 1-benzyl-1H-1,2,3-triazole derivatives of carbohydrates. *Eur J Med Chem*, 44(1), 373-383.

- Dufour, E., Roger, P., & Haertle, T. (1992). Binding of Benzo(α)pyrene, Ellipticine, and Cis-Parinaric Acid to β -Lactoglobulin: Influence of Protein Modifications. *Journal of Protein Chemistry*, 11(6), 645-652.
- Ghosh, J., Swarup, V., Saxena, A., Das, S., Hazra, A., Paira, P., . . . Basu, A. (2008). Therapeutic effect of a novel anilidoquinoline derivative, 2-(2-methyl-quinoline-4ylamino)-N-(2-chlorophenyl)-acetamide, in Japanese encephalitis: correlation with in vitro neuroprotection. *Int J Antimicrob Agents*, 32(4), 349-354.
- Jr., I. T., Sauer, K., Wang, J. C., Puglisi, J. D., Harbison, G., & Rovnyak, D. (2002). *Physical Chemistry: Principles and Applications in Biological Sciences* (4 ed.). New Jersey: Prentice Hall, inc.
- Khodarahmi, R., Karimi, S. A., Ashrafi Kooshk, M. R., Ghadami, S. A., Ghobadi, S., & Amani, M. (2012). Comparative spectroscopic studies on drug binding characteristics and protein surface hydrophobicity of native and modified forms of bovine serum albumin: possible relevance to change in protein structure/function upon non-enzymatic glycation. *Spectrochim Acta A Mol Biomol Spectrosc*, 89, 177-186.
- Kumar, S., Bawa, S., Drabu, S., & Panda, B. P. (2010). Design and synthesis of 2-chloroquinoline derivatives as non-azoles antimycotic agents. *Medicinal Chemistry Research*, 20(8), 1340-1348.
- Lleres, D., Swift, S., & Lamond, A. I. (2007). Detecting protein-protein interactions in vivo with FRET using multiphoton fluorescence lifetime imaging microscopy (FLIM). *Curr Protoc Cytom, Chapter 12, Unit12 10*.
- Lou, Y.-Y., Zhou, K.-L., Pan, D.-Q., Shen, J.-L., & Shi, J.-H. (2017). Spectroscopic and molecular docking approaches for investigating conformation and binding characteristics of clonazepam with bovine serum albumin (BSA). *Journal of Photochemistry and Photobiology B: Biology*, 167, 158-167.
- Madapa, S., Tusia, Z., D.Sridhar, A.Kumar, M.I.Siddiqi, K.Srivastava, . . . S.Batra. (2009). Search for new pharmacophores for antimalarial activity. Part I: Synthesis and

- antimalarial activity of new 2-methyl-6-ureido-4-quinolinamides. *Bioorganic & Medicinal Chemistry*, 17, 203–221.
- Makarasen, A., Kuno, M., Patnin, S., Reukngam, N., Khlaychan, P., Deeyohe, S., . . . Techasaku, S. (2019). Molecular Docking Studies and Synthesis of Amino-oxydiarylquinoline Derivatives as Potent Non-nucleoside HIV-1 Reverse Transcriptase Inhibitors. *Drug Research*, 69, 671-682.
- Narayan Acharya, B., Thavaselvam, D., & Parshad Kaushik, M. (2008). Synthesis and antimalarial evaluation of novel pyridine quinoline hybrids. *Medicinal Chemistry Research*, 17(8), 487-494.
- Owen, T. (1996). *Fundamentals of Modern UV-Visible Spectroscopy : A Primer*: Hewlett-Packard
- Patnin, S., Makarasenb, A., Kuno, M., Deeyohe, S., Techasakul, S., & Chaivisuthangkura, A. (2020). Binding interaction of potent HIV-1 NNRTIs, amino-oxy-diarylquinoline with the transport protein using spectroscopic and molecular docking. *Spectrochimica Acta Part A: Molecular and Biomolecular Spectroscopy*, 233, 118159.
- Paul, B. K., Guchhait, N., & Bhattacharya, S. C. (2017). Binding of ciprofloxacin to bovine serum albumin: Photophysical and thermodynamic aspects. *J Photochem Photobiol B*, 172, 11-19.
- Raynes, K., Foley, M., Tilley, L., & Deady, L. W. (1996). Novel bisquinoline antimalarials: Synthesis, antimalarial activity, and inhibition of haem polymerization. *Biochemical Pharmacology*, 52, 551-559.
- Ross, P. D., & Subramanian, S. (1981a). Thermodynamics of Protein Association Reactions: Forces Contributing to Stability. *THERMODYNAMICS OF PROTEIN ASSOCIATION*, 20, 3096-3102.
- Ross, P. D., & Subramanian, S. (1981b). Thermodynamics of protein association reactions: forces contributing to stability. *Biochemistry*, 20(11), 3096-3102.
- Russell, P. (2010). *iGenetics* (3 ed.): Steven M. Carr.

- Sarkar, M., Paul, S. S., & Mukherjea, K. K. (2013). Interaction of bovine serum albumin with a psychotropic drug alprazolam: Physicochemical, photophysical and molecular docking studies. *Journal of Luminescence*, *142*, 220-230.
- Scott, D. A., Balliet, C. L., Cook, D. J., Davies, A. M., Gero, T. W., Omer, C. A., . . . Zinda, M. J. (2009). Identification of 3-amido-4-anilinoquinolines as potent and selective inhibitors of CSF-1R kinase. *Bioorg Med Chem Lett*, *19*(3), 697-700.
- Seery, M., Fay, N., McCormac, T., Dempsey, E., Forster, R., & Keyes, T. (2005). Photophysics of Ruthenium Polypyridyl Complexes formed with lacunary polyoxotungstates with iron addenda. *Physical Chemistry Chemical Physics*, *19*(7), 3426 – 3433.
- Shahabadi, N., Khorshidi, A., & Moghadam, N. H. (2013). Study on the interaction of the epilepsy drug, zonisamide with human serum albumin (HSA) by spectroscopic and molecular docking techniques. *Spectrochim Acta A Mol Biomol Spectrosc*, *114*, 627-632.
- Shi, J. H., Chen, J., Wang, J., Zhu, Y. Y., & Wang, Q. (2015). Binding interaction of sorafenib with bovine serum albumin: Spectroscopic methodologies and molecular docking. *Spectrochim Acta A Mol Biomol Spectrosc*, *149*, 630–637.
- Tremblay, M., Bethell, R. C., Cordingley, M. G., DeRoy, P., Duan, J., Duplessis, M., . . . Sturino, C. F. (2013). Identification of benzofurano[3,2-d]pyrimidin-2-ones, a new series of HIV-1 nucleotide-competing reverse transcriptase inhibitors. *Bioorg Med Chem Lett*, *23*(9), 2775-2780.
- Upadhyaya, R. S., Vandavasi, J. K., Vasireddy, N. R., Sharma, V., Dixit, S. S., & Chattopadhyaya, J. (2009). Design, synthesis, biological evaluation and molecular modelling studies of novel quinoline derivatives against Mycobacterium tuberculosis. *Bioorg Med Chem*, *17*(7), 2830-2841.
- Ware, W. R. (1962). Oxygen Quenching of Fluorescence in Solution: An Experimental Study of the Diffusion Process. *The Journal of Physical Chemistry*, *66*(3), 455-458.

- Wei, B. Q., Weaver, L. H., Ferrari, A. M., Matthews, B. W., & Shoichet, B. K. (2004). Testing a flexible-receptor docking algorithm in a model binding site. *J Mol Biol*, 337(5), 1161-1182.
- Wu, X., Liu, J., Wang, Q., Xue, W., Yao, X., Zhang, Y., & Jin, J. (2011). Spectroscopic and molecular modeling evidence of clozapine binding to human serum albumin at subdomain IIA. *Spectrochim Acta A Mol Biomol Spectrosc*, 79(5), 1202-1209.
- Xu, L., Hu, Y.-X., Li, Y.-C., Zhang, L., Ai, H.-X., Liu, H.-S., . . . Sang, Y.-L. (2017). Study on the interaction of tussilagone with human serum albumin (HSA) by spectroscopic and molecular docking techniques. *Journal of Molecular Structure*, 1149, 645-654.
- Zheng, M., Liu, X., Xu, Y., Li, H., Luo, C., & Jiang, H. (2013). Computational methods for drug design and discovery: focus on China. *Trends Pharmacol Sci*, 34(10), 549-559.



VITA

NAME Suwicha Patnin

DATE OF BIRTH 15 November 1989

PLACE OF BIRTH Thailand

INSTITUTIONS ATTENDED Bachelor's Degree, Chemistry, Srinakharinwirot university
Master degree, Chemistry, Srinakharinwirot university

HOME ADDRESS 22/8 Moo 3 District Sing Amphoe Bang Rachan Province
Singburi 16130

PUBLICATION Binding interaction of potent HIV-1 NNRTIs, amino-oxy-diarylquinoline with the transport protein using spectroscopic and molecular docking

